Research Paper

Long-term $PM_{2.5}$ exposure increases the risk of non-small cell lung cancer (NSCLC) progression by enhancing interleukin-17a (IL-17a)-regulated proliferation and metastasis

Xie Chao[1,*], Liu Yi[2,*], Li Lan Lan[3,*], Han Yun Wei[4,*], Dong Wei[1]

[1]Department of Oncology, Shandong Cancer Hospital and Institute, Shandong First Medical University and Shandong Academy of Medical Sciences, Jinan 250117, Shandong Province, P.R. China
[2]Centers of Disease Control and Prevention of Shandong Province, Jinan 250014, Shandong Province, P.R. China
[3]Affiliated Hospital of Binzhou Medical College, Binzhou 256603, Shandong Province, P.R. China
[4]Department of Oncology, Affiliated Hospital of Southwest Medical University, Luzhou 646000, Sichuan Province, P.R. China
*Equal contribution

Correspondence to: Dong Wei; **email:** mddou.xu.1979@qq.com
Keywords: PM2.5, NSCLC, IL-17a, EMT, metastasis
Received: February 11, 2020 **Accepted:** April 28, 2020 **Published:** June 18, 2020

ABSTRACT

$PM_{2.5}$ is a class of airborne particles and droplets with sustained high levels in many developing countries. Epidemiological studies have indicated that $PM_{2.5}$ is closely associated with the increased morbidity and mortality of lung cancer in the world. Unfortunately, the effects of $PM_{2.5}$ on lung cancer are largely unknown. In the present study, we attempted to explore the role of $PM_{2.5}$ in the etiology of NSCLC. Here, we found that long-term $PM_{2.5}$ exposure led to significant pulmonary injury. Epithelial-mesenchymal transition (EMT) and cancer stem cells (CSC) properties were highly induced by $PM_{2.5}$ exposure. EMT was evidenced by the significant up-regulation of MMP2, MMP9, TGF-β1, α-SMA, Fibronectin and Vimentin. Lung cancer progression was associated with the increased expression of Kras, c-Myc, breast cancer resistance protein BCRP (ABCG2), OCT4, SOX2 and Aldh1a1, but the decreased expression of p53 and PTEN. Importantly, mice with IL-17a knockout (IL-17a$^{-/-}$) showed significantly alleviated lung injury and CSC properties following $PM_{2.5}$ exposure. Also, IL-17a$^{-/-}$-attenuated tumor growth was recovered in $PM_{2.5}$-exposed mice injected with recombinant mouse IL-17a, accompanied with significantly restored lung metastasis. Taken together, these data revealed that $PM_{2.5}$ could promote the progression of lung cancer by enhancing the proliferation and metastasis through IL-17a signaling.

INTRODUCTION

Particulate matter (PM) is a class of air pollutants, and consists of airborne solid particles and liquid droplets [1]. PM pollution has been one of the highest risk factor among various researched factors in the world [2]. $PM_{2.5}$ is characterized as the particles and droplets with aerodynamic diameter ≤ 2.5 μm [3]. Epidemiological studies have indicated that the increasingly serious air pollution and $PM_{2.5}$ levels are closely associated with health-related issues, including the enhanced hospitalization, increased mortality and mortality because of respiratory problems, shortened lifespan due to long-term $PM_{2.5}$ exposure, as well as the up-regulated incidence and severity of lung cancer [4–6]. Some potential molecular mechanisms have been involved in the progression of lung injury triggered by $PM_{2.5}$ exposure, including excessive oxidative stress, pro-inflammatory response and apoptotic cell death [7–9]. Recently, more and more studies have reported the potential of $PM_{2.5}$ in increasing the risk of lung cancer [10, 11]. In addition, there were reports that

demonstrated that the decreased exposure to cigarette smoking attenuated the incidence of lung cancer in the West [4, 7], underlying the importance of air pollution for lung cancer progression. However, little research has focused on the molecular mechanisms. Lung cancer is one of the most common malignancies worldwide and a major reason for tumor-associated death [12, 13]. As reported, NSCLC accounts for approximately 80% of all lung cancer cases, which includes adenocarcinoma and squamous cell carcinoma [14]. The 5-year survival rate of NSCLC is still less than 15%, which is related to the highly malignant potential and the lack of obvious symptoms for early diagnosis [15, 16]. Elevated ability of motility and proliferation were observed in NSCLC cells following $PM_{2.5}$ exposure [17]. In human lung cancer cells, EMT could also be promoted after $PM_{2.5}$ exposure [18]. Furthermore, lung cancer stem cell properties induced by chronic $PM_{2.5}$ exposure has also been reported [19]. Nevertheless, the molecular mechanism by which $PM_{2.5}$ exposure contributes to NSCLC has not been well investigated. It is necessary to thoroughly investigate the mechanisms in NSCLC after exposure to particulate matter to better characterize gene-environment interactions and epigenetic influences on cancer exacerbation.

Interleukin-17 (IL-17) is produced by Th17 cells and other cells, such as $CD8^+$ T cells, γδ T cells, mast cells, invariant NKT cells, and granulocytes [20]. IL-17 plays an essential role in regulating inflammatory and autoimmune diseases [21]. Up-regulated IL-17-producing Th17 cells have been indicated in a variety of human carcinoma cases [22, 23]. For instance, the proportion of Th17 cells was elevated within the peripheral blood and tumor tissues of esophageal cancer patients [24]. Tumor-infiltrating Th17 cells were detected in human colorectal cancer, which were associated with shortened disease-free survival [25]. In addition, IL-17 might be implicated in the metastasis of NSCLC through promoting lymphangiogenesis [26]. Recent analysis also indicated that IL-17 might be a critical cytokine involved in the progression of NSCLC. Both *in vivo* and *in vitro* experiments showed that IL-17 could directly enhance the invasion of NSCLC cells [27, 28]. These findings revealed the potential of IL-17 in the promoting the development of NSCLC. IL-17a is one of six members (A-F) of the IL-17 family [29, 30]. In a recent study, the increased expression of IL-17a in the lung of patients with lung adenocarcinoma was reported. Local suppression of IL-17a in the lung of a model with lung cancer showed improved anti-tumor immunity featured by the enhanced IFNγ, a reduced number of T-regulatory cell and the inhibited tumor growth [31]. Although previous studies have illustrated the potential of IL-17a during lung cancer progression, its effects on NSCLC induced by $PM_{2.5}$ have little to be reported.

In this present study, we aimed to further explore the effects of $PM_{2.5}$ on NSCLC progression, as well as its relationship with IL-17a expression change by the *in vivo* and *in vitro* experiments. Here, we showed that long-term $PM_{2.5}$ exposure led to lung injury and CSC properties. IL-17a expression levels were significantly up-regulated by $PM_{2.5}$ in pulmonary tissues, peripheral blood lymphocytes and splenic lymphocytes. NSCLC patients exhibited higher IL-17a expression. In NSCLC cells, $PM_{2.5}$ was discovered to promote the cell proliferation, migration and invasion through up-regulating IL-17a expression levels. Importantly, we for the first time found that IL-17a knockout markedly alleviated $PM_{2.5}$-induced lung injury and CSC properties. Of note, the animal studies showed that $PM_{2.5}$-enhanced tumor growth was clearly abolished by IL-17a knockout in the established tumor xenograft models. Additionally, results by *in vivo* tumor metastasis confirmed that IL-17a knockout inhibited metastasis in $PM_{2.5}$-challenged mice. Therefore, our results demonstrated that $PM_{2.5}$ could elevate the proliferation and metastasis via increasing IL-17a expression levels, accelerating NSCLC progression consequently.

RESULTS

$PM_{2.5}$ treatments result in pulmonary injury and fibrosis

In order to investigate the effects of $PM_{2.5}$ on NSCLC progression, the pulmonary condition in mice with long-term $PM_{2.5}$ exposure was firstly calculated. Histopathological analysis of lung sections using H&E and Masson staining demonstrated that $PM_{2.5}$ treatment for 3 months caused more severe injury and fibrosis than the FA mice (Figure 1A). Compared to the FA group, $PM_{2.5}$ markedly increased total protein levels in BALF in a time-dependent manner (Figure 1B). Similarly, the number of total cells and neutrophils were significantly increased in mice exposed to $PM_{2.5}$, indicating the critical inflammation in mice (Figure 1C, 1D). EMT is an important process that contributes to fibrogenesis [32]. Then, fibrosis- and/or EMT-associated genes, including MMP2, MMP9, TGF-β1, α-SMA, Fibronectin and Vimentin [33, 34], in lung samples of mice were highly induced by $PM_{2.5}$ administration in a time-dependent manner (Figure 1E). Both serum and lung TNF-α and IL-6 expression levels were greatly up-regulated in $PM_{2.5}$-challenged mice (Figure 1F, 1G). These results showed that long-term $PM_{2.5}$ exposure led to severe pulmonary injury in mice.

$PM_{2.5}$ treatments lead to cancer stem cell properties in mice

EMT is a critical event that is often activated during the process of tumor invasion and metastasis. It is also an

important and potential driving factor for cancer initiation and development [35]. Then, the lung cancer markers and cancer stem cell features of lung cells (Kras, c-Myc, ABCG2, OCT4, SOX2 and Aldh1a1) [18, 36–38], and the tumor suppressor genes (p53 and PTEN) [39] were calculated using RT-qPCR and/or immunohistochemistry (IHC) staining. As shown in Figure 2A, 2B, Kras, c-Myc, ABCG2, OCT4, SOX2 and Aldh1a1 expression levels were highly induced in pulmonary samples from $PM_{2.5}$-treated mice compared with the FA group. In contrast, $PM_{2.5}$ exposure time-dependently reduced the expression of p53 and PTEN. These results demonstrated that $PM_{2.5}$ long-term exposure could result in the cancer stem cell properties *in vivo*.

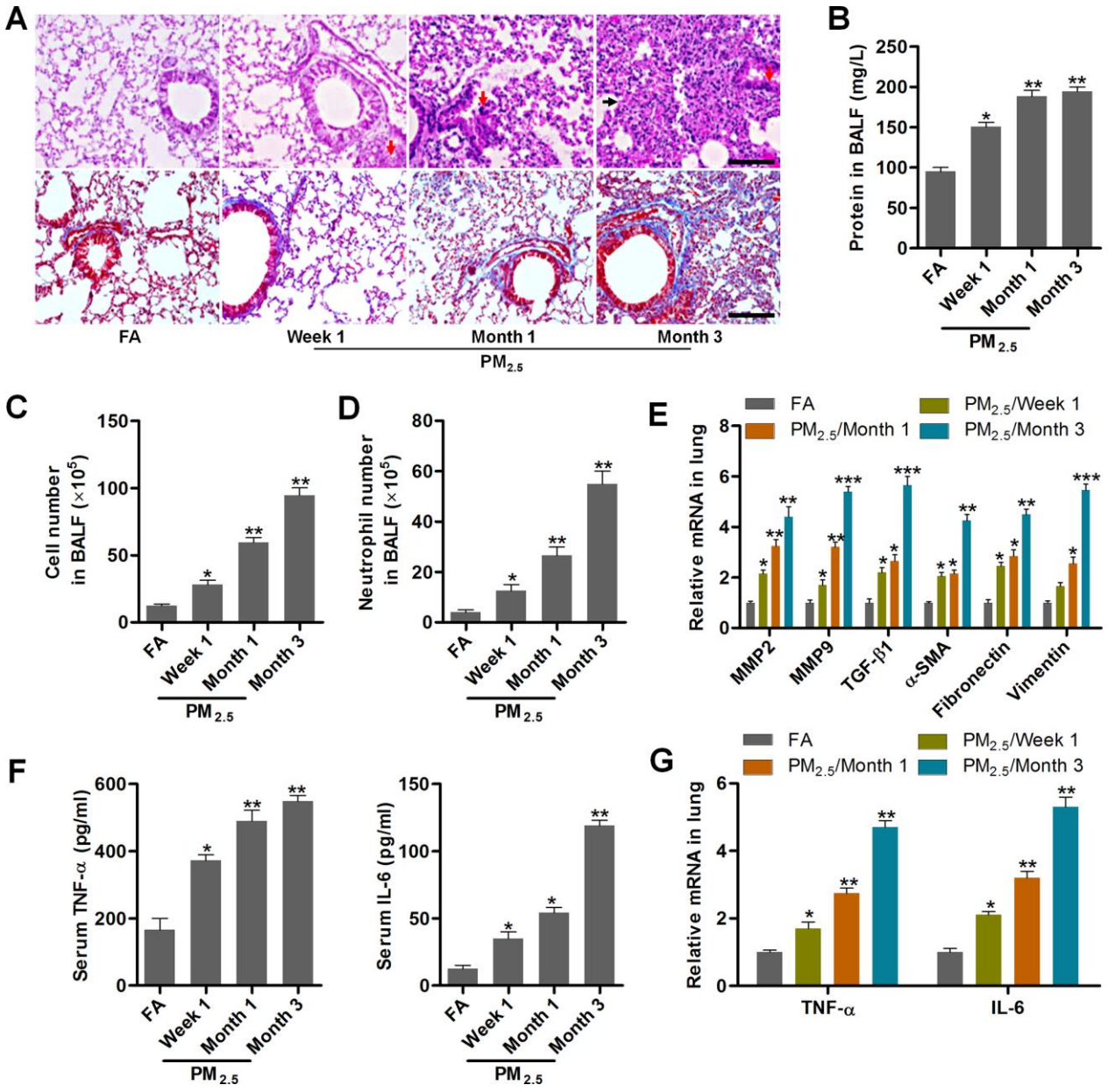

Figure 1. $PM_{2.5}$ treatments result in pulmonary injury and fibrosis. (**A**) H&E staining (up panel) and Masson trichrome staining (down panel) of lung sections from mice challenged with $PM_{2.5}$ for the indicated time points (n = 6). Scale bar, 100 μm. (**B**) Protein contents in the BALF were measured in mice treated with $PM_{2.5}$ at the indicated time (n = 8). The number of (**C**) total cells and (**D**) neutrophils of BALF were calculated in $PM_{2.5}$-challenged mice at the indicated time (n = 8). (**E**) RT-qPCR analysis of genes associated with fibrosis, including MMP2, MMP9, TGF-β1, α-SMA, Fibronectin and Vimentin, in lung samples of $PM_{2.5}$-treated mice (n = 4). (**F**) TNF-α and IL-6 levels in serum of $PM_{2.5}$-challenged mice were determined by ELISA (n = 8). (**G**) RT-qPCR analysis was used to assess TNF-α and IL-6 mRNA expression levels in pulmonary samples of mice treated with $PM_{2.5}$ for the indicated time (n = 4). All data are expressed as mean ± SEM. $^{*}p<0.05$, $^{**}p<0.01$ and $^{***}p<0.001$ compared to the FA group.

$PM_{2.5}$ enhances IL-17a expression in mice

IL-17a has pro-tumor actions, which is associated with angiogenesis [24, 40]. In our study, we found that IL-17a contents in BALF and in serum of mice were markedly increased by $PM_{2.5}$ challenge (Figure 3A, 3B). Higher expression of IL-17a both from mRNA and protein levels were observed in pulmonary samples of mice exposed to $PM_{2.5}$ (Figure 3C–3E). Consistently, ELISA results showed that IL-17a levels in the peripheral blood

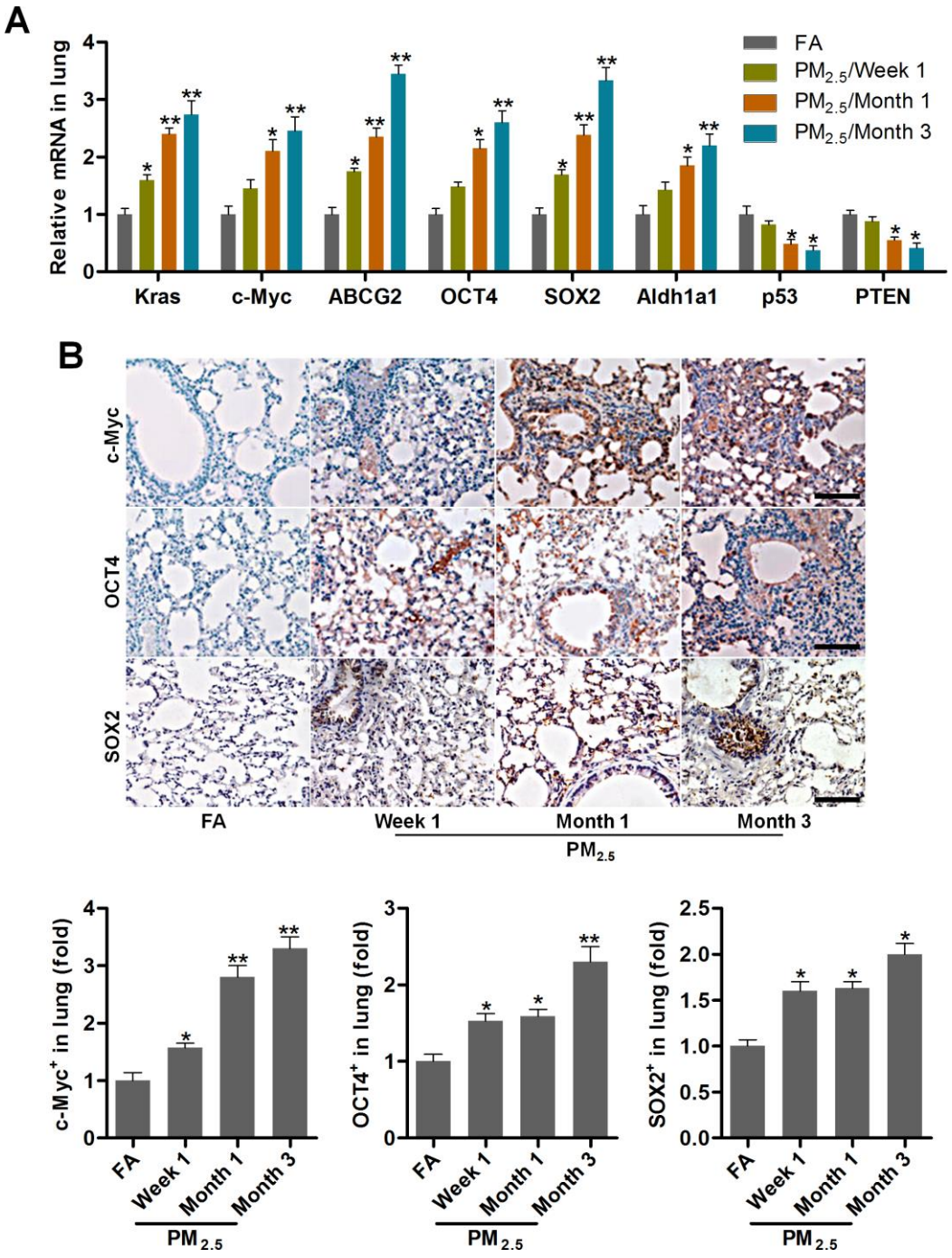

Figure 2. $PM_{2.5}$ treatments lead to cancer stem cell properties in mice. (**A**) RT-qPCR analysis was used to measure lung cancer-related biomarkers (Kras, c-Myc, ABCG2, OCT4, SOX2, Aldh1a1, p53 and PTEN) in lung tissues of mice following $PM_{2.5}$ treatment at the indicated time (n = 4). (**B**) IHC staining was performed to calculate c-Myc, OCT4 and SOX2 in pulmonary sections of $PM_{2.5}$-challenged mice (n = 6). The quantification of c-Myc, OCT4 and SOX2 relative expression was exhibited. Scale bar, 100 μm. All data are expressed as mean ± SEM. *$^{*}p<0.05$* and *$^{**}p<0.01$* compared to the FA group.

lymphocytes and in splenic lymphocytes were markedly up-regulated in $PM_{2.5}$-treated mice compared to the FA group (Figure 3F, 3G). Together, findings above indicated that $PM_{2.5}$ exposure could promote IL-17a expression, which might be involved in the initiation and progression of lung cancer.

IL-17a expression is up-regulated in patients with lung cancer

To confirm the regulatory role of IL-17a potentiated by $PM_{2.5}$ during lung cancer development, here the expression change of IL-17a in patients with lung cancer was at first explored. As shown in Figure 4A, an obvious up-regulation of IL-17a in the lung cancer tissues compared to the normal tissues was detected by IHC staining, and IL-17a expression was found to be positively correlated with lung cancer progression. RT-qPCR and western blotting analysis also demonstrated that IL-17a expression levels were higher in lung cancer samples compared to the adjacent normal tissues (Figure 4B, 4C). We also found that patients with low IL-17a expression exhibited better overall survival rates than that of the group with high IL-17a expression

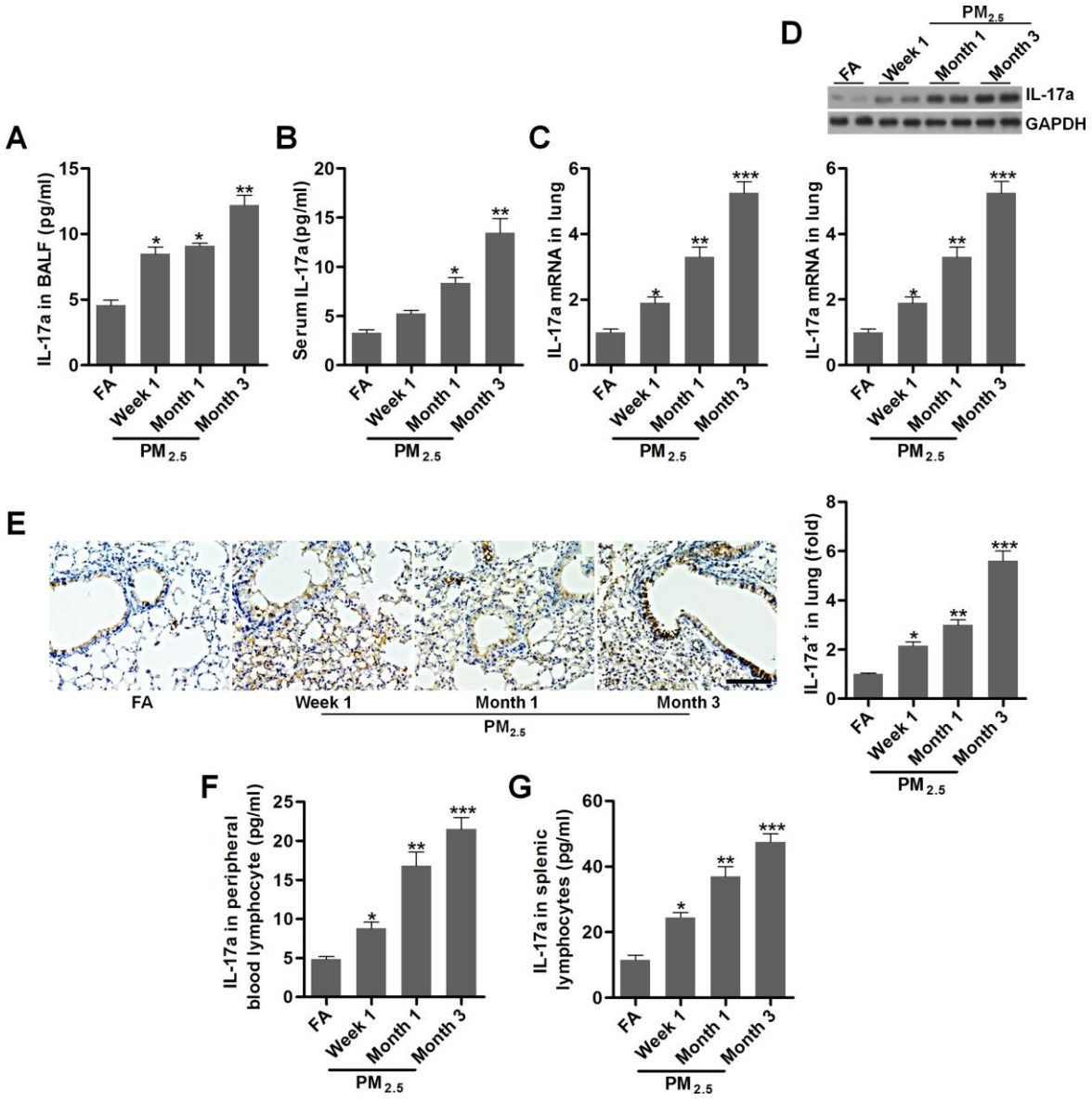

Figure 3. $PM_{2.5}$ enhances IL-17a expression in mice. (**A**, **B**) IL-17a contents in BALF and serum were measured by ELISA, respectively (n = 8). (**C**) RT-qPCR, (**D**) western blotting and (**E**) IHC analysis of IL-17a in lung tissues of mice challenged with $PM_{2.5}$ for the indicated time (n = 6). Scale bar, 100 μm. (**F**, **G**) IL-17a levels in the peripheral blood lymphocytes and in splenic lymphocytes were calculated using ELISA analysis (n = 8). All data are expressed as mean ± SEM. *$p<0.05$, **$p<0.01$ and ***$p<0.001$ compared to the FA group.

(Figure 4D). These results indicated that IL-17a increase was associated with poor clinical outcomes of patients with lung cancer.

$PM_{2.5}$ elevates the proliferation in NSCLC cells

To confirm the effects of $PM_{2.5}$ on NSCLC, the *in vitro* experiments using A549 and H1299 were performed. At first, we found that $PM_{2.5}$ exposure led to significant up-regulation of TNF-α and IL-6 in the supernatants of Th17 cells compared to the Control group (Figure 5A). Higher IL-17a contents in supernatants collected from $PM_{2.5}$-exposed Th17 cells were observed (Figure 5B). In addition, IL-17a expression levels in Th17 cells were also markedly increased by $PM_{2.5}$ treatment in comparison to the Control group (Figure 5C–5E). Results above showed that $PM_{2.5}$ could up-regulate IL-17a expression levels in Th17 cells.

Then, NSCLC cell lines of A549 and H1299 were incubated in the culture medium composed of the fresh medium and the conditional medium from Th17 cells with or without $PM_{2.5}$ stimulation at 3:1. CCK-8 analysis showed that A549 and H1299 cells cultured in medium from Th17 cells with $PM_{2.5}$ treatment exhibited higher cell proliferative activity (Figure 5F). Similar proliferative trends were observed in A549 and H1299 cells by the colony formation and EdU assays (Figure 5G, 5H). These results demonstrated that $PM_{2.5}$ exposure could promote the proliferation of NSCLC cells.

$PM_{2.5}$ contributes to the migration and invasion of NSCLC cells

We next explored the effect of $PM_{2.5}$ exposure on NSCLC cell migration and invasion. A549 and H1299 cells have high migratory and invasive abilities [41]. Under $PM_{2.5}$-exposed circumstances, A549 and H1299 cells had higher migration and invasion compared to the control group by transwell analysis (Figure 6A–6C). Wound healing analysis confirmed that $PM_{2.5}$ exposure

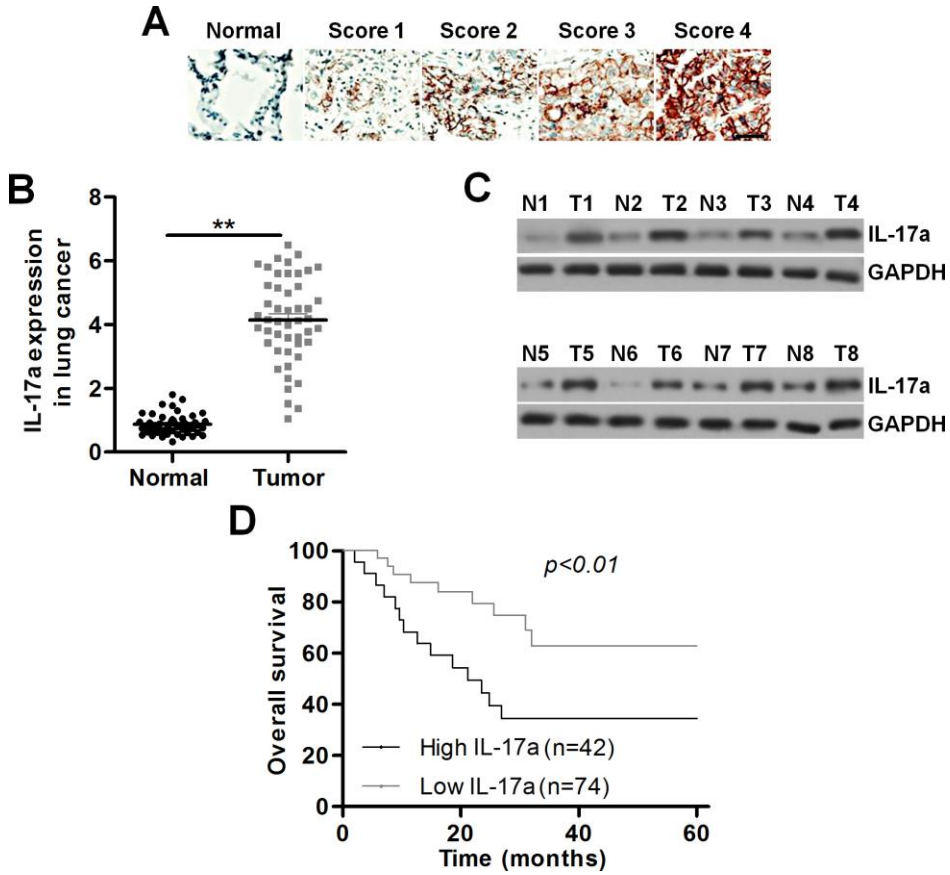

Figure 4. IL-17a expression is up-regulated in patients with lung cancer. (**A**) Images showing IL-17a expression levels in tumor samples from patients with lung cancer using IHC. Scale bar, 100 μm. (**B**) IL-17a expression levels in the primary lung tumor specimens and the adjacent normal tissue samples by RT-qPCR (n = 48). (**C**) Western blot analysis of IL-17a expression levels in the primary lung tumor specimens and the paired lung alveolar tissue samples (n = 8). (**D**) Kaplan-Meier survival curves for overall survival (OS) in lung cancer patients according to the expression levels of IL-17a. All data are expressed as mean ± SEM. $^{**}p<0.01$.

enhanced the migration of cells compared with the untreated control cells (Figure 6D, 6E). Moreover, the mRNA expression levels of EMT-associated genes including MMP2, MMP9, TGF-β1, α-SMA, Fibronectin and Vimentin were markedly up-regulated in NSCLC cells cultured in medium containing supernatants from $PM_{2.5}$-incubated Th17 cells (Figure 6F). IF staining further demonstrated that the conditional medium from $PM_{2.5}$-treated Th17 cells led to the expression of N-cadherin in A549 and H1299 cells (Figure 6G).

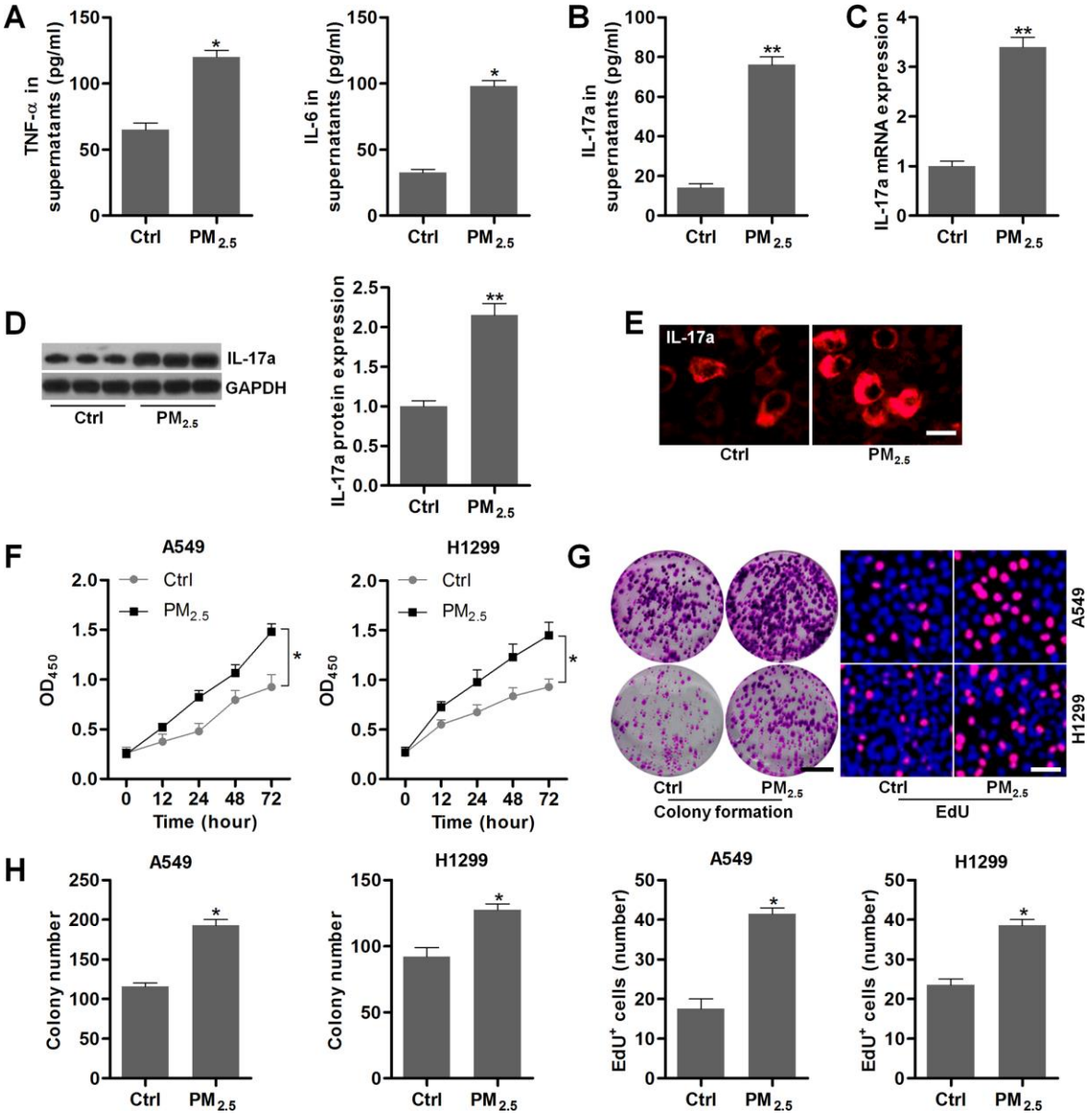

Figure 5. $PM_{2.5}$ elevates the proliferation in NSCLC cells. (**A**–**E**) Th17 cells were treated with 100 μg/cm² of $PM_{2.5}$ for 24 h, and then all cells and supernatants were collected for the analysis. (**A**) TNF-α and IL-6 levels in the supernatants were measured using ELISA. (**B**) IL-17a contents in the collected supernatants were calculated using ELISA. (**C**) RT-qPCR and (**D**) western blot analysis were used to measure IL-17a expression levels in the harvested cells. (**E**) IF staining of IL-17a in the harvested cells. Scale bar, 20 μm. (**F**) Th17 cells were treated with 100 μg/cm² of $PM_{2.5}$ for 24 h, and then the conditional medium was collected, and mixed with fresh RPMI1640 absolute medium at 1:3. The composed culture medium was exposed to A549 and H1350 cells for 12, 24, 48 or 72 h. Then, the NSCLC cells were collected for cell proliferation analysis using CCK-8 analysis. (**G**, **H**) Th17 cells were incubated with 100 μg/cm² of $PM_{2.5}$ for 24 h, and then the conditional medium was collected, and mixed with fresh RPMI1640 absolute medium at 1:3. Then, the composed culture medium was subjected to A549 and H1350 cells for another 24 h. Subsequently, all cells were harvested to assess the cell proliferation using colony formation and EdU assays. Scale bar, 100 μm. Quantification of colony formation assay and EdU was exhibited. All data are expressed as mean ± SEM. $^{*}p<0.05$ and $^{**}p<0.01$ compared to the Ctrl group.

Collectively, the results in this section demonstrated that $PM_{2.5}$-induced circumstances could accelerate EMT in NSCLC.

IL-17a treatment promotes the proliferation and EMT in NSCLC cells

To further confirm the effects of IL-17a on NSCLC progression, Recombinant Human IL-17a was then subjected to A549 and H1299 cells. CCK-8 analysis demonstrated that IL-17a treatment markedly promoted the proliferation of NSCLC cells (Figure 7A). Colony formation and EdU assays confirmed the role of IL-17a in promoting NSCLC proliferation (Figure 7B, 7C). Transwell analysis demonstrated that the number of cells in migration and invasion was markedly up-regulated by IL-17a addition (Figure 7D, 7E). Furthermore, MMP2, MMP9, TGF-β1, α-SMA, Fibronectin and Vimentin

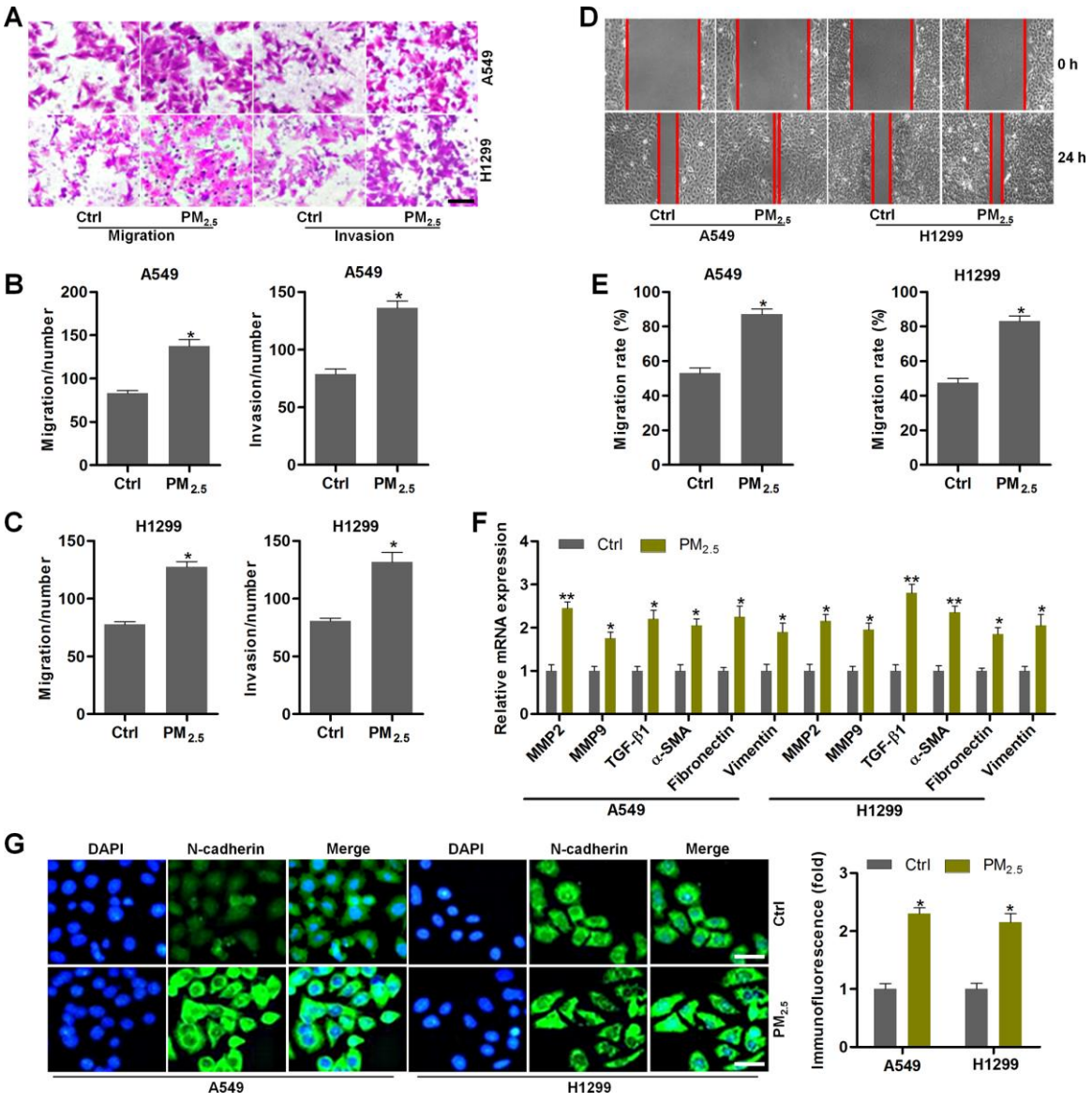

Figure 6. $PM_{2.5}$ contributes to the migration and invasion of NSCLC cells. (**A**–**G**) Th17 cells were exposed to 100 μg/cm² of $PM_{2.5}$ for 24 h. Then, the obtained medium was collected, and mixed with fresh RPMI1640 absolute medium at 1:3 dilutions. Next, A549 and H1350 cells were treated with the composed culture medium for another 24 h. Subsequently, all cells were collected for the following analysis. (**A**) Transwell analysis was used to determine the migration and invasion of lung cancer cells. Scale bar, 100 μm. (**B**, **C**) Quantification of the number of cells in migration and invasion. (**D**) Wound healing analysis was performed to assess the migration of lung cancer cells. (**E**) The number of NSCLC cells in migration was quantified following wound healing analysis. (**F**) RT-qPCR analysis was used to calculate the mRNA expression levels of genes associated with EMT. (**G**) IF staining of N-cadherin in A549 and H1350 cells treated as indicated. Scale bar, 50 μm. All data are expressed as mean ± SEM. *$p<0.05$ and **$p<0.01$ compared to the Ctrl group.

mRNA levels were significantly induced by IL-17a in A549 and H1299 cells (Figure 7F). The role of IL-17a in promoting N-cadherin was verified by IF staining as displayed in Figure 7G. Together, results in this regard illustrated that IL-17a could enhance the proliferation and EMT in NSCLC.

IL-17a knockout alleviates pulmonary injury and cancer stem cell properties in mice following $PM_{2.5}$ exposure for 3 months

The *in vivo* and *in vitro* experiments above demonstrated that $PM_{2.5}$ could up-regulate IL-17a expression to

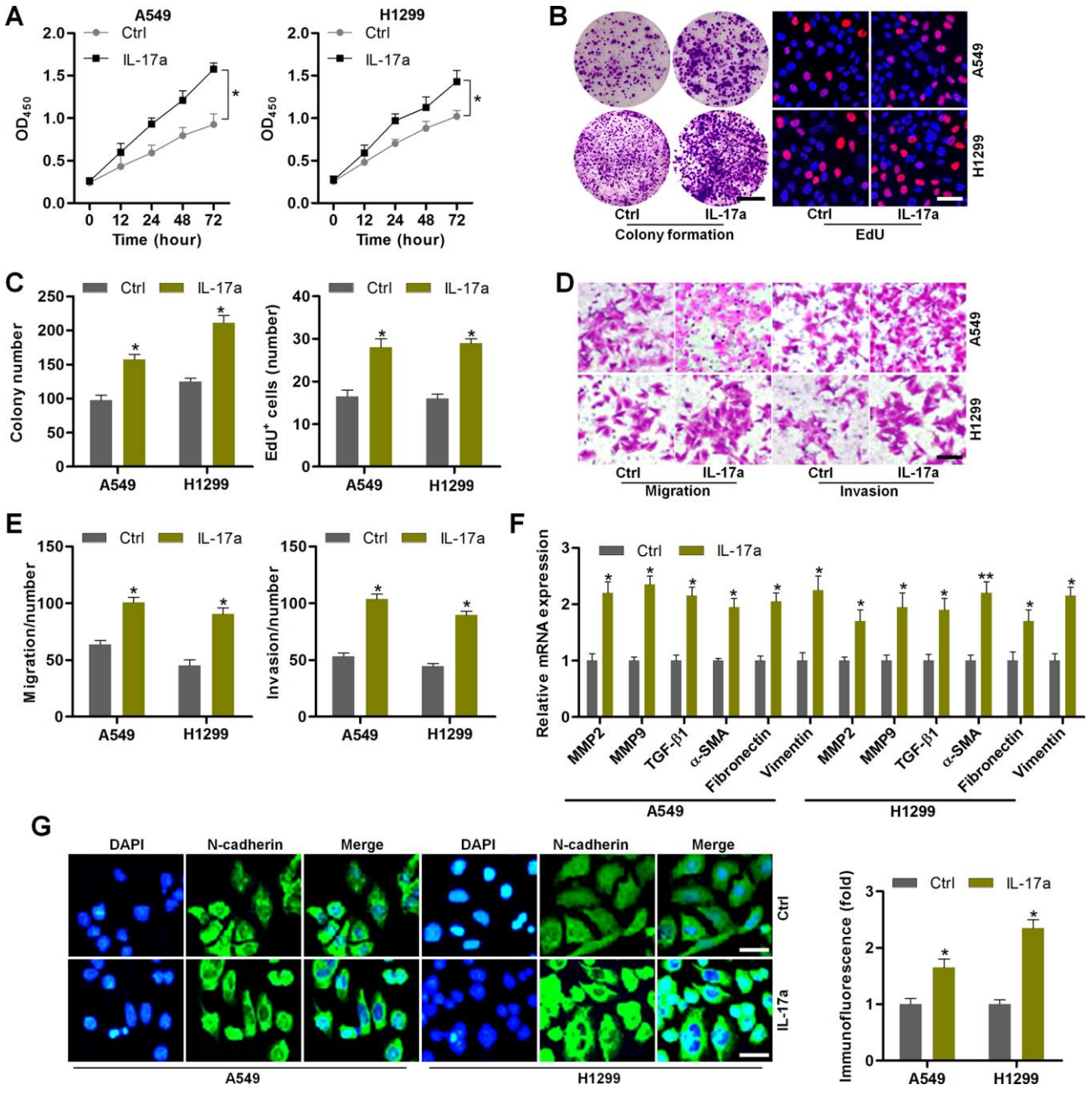

Figure 7. IL-17a treatment promotes the proliferation and EMT in NSCLC cells. (**A**–**G**) A549 and H1350 cells were treated with or without IL-17a (100 ng/ml) for 24 h, and then were collected for the following studies. (**A**) CCK-8 analysis was used to determine the cell proliferative activity. (**B**) Colony formation and EdU assays were used to determine the cell proliferative condition. Scale bar, 100 μm. (**C**) Quantification of the number of cells by colony formation and EdU analysis. (**D**) Transwell analysis was used to calculate the number of cells in migration and invasion. Scale bar, 100 μm. (**E**) Quantification of the counts of the migrated and invaded cells. (**F**) RT-qPCR analysis was used to measure EMT-associated genes in A549 and H1350 cells. (**G**) IF staining of N-cadherin in A549 and H1350 cells. Scale bar, 50 μm. All data are expressed as mean ± SEM. $^{*}p<0.05$ and $^{**}p<0.01$ compared to the Ctrl group.

subsequently promote the progression of NSCLC via enhancing the proliferation and EMT processes. In order to further confirm the significant role of IL-17a regulated by $PM_{2.5}$ in pulmonary progression and lung cancer development, IL-17a knockout (IL-17a$^{-/-}$) mice were used subsequently. As shown in Figure 8A, H&E and Masson staining showed that $PM_{2.5}$-induced pulmonary injury and fibrosis were attenuated when IL-17a was deleted in mice. Total proteins in BALF induced by long-term $PM_{2.5}$ exposure were significantly

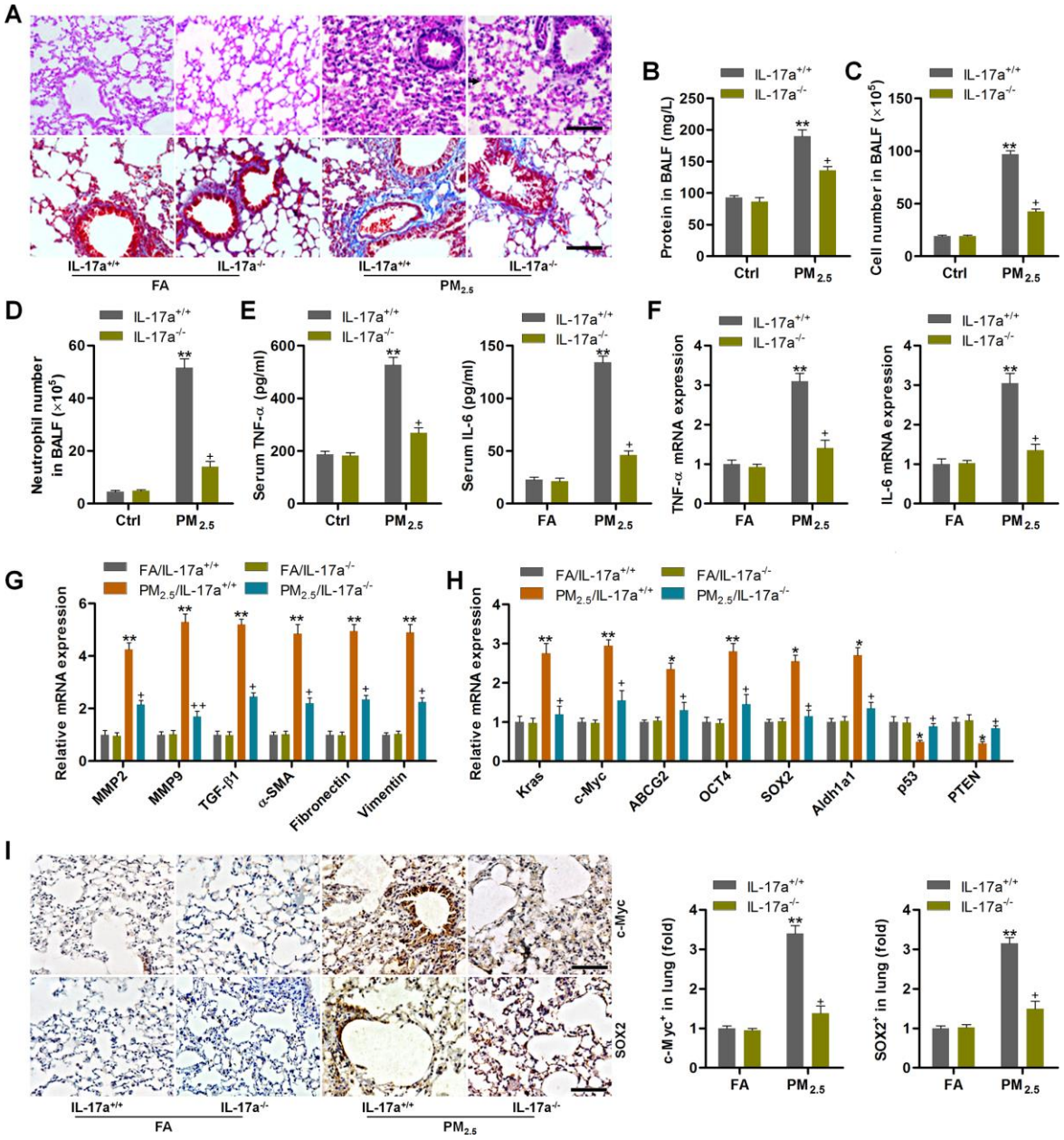

Figure 8. IL-17a knockout alleviates pulmonary injury and cancer stem cell properties in mice following $PM_{2.5}$ exposure for 3 months. (**A**) H&E staining (up panel) and Masson trichrome staining (down panel) of lung sections from IL-17a$^{+/+}$ and IL-17a$^{-/-}$ mice challenged with or without $PM_{2.5}$ for 3 months (n = 6). Scale bar, 100 μm. (**B**) Protein levels in BALF were measured (n = 8). (**C**) The total number of cells in BALF was assessed (n = 8). (**D**) The number of neutrophils in BALF was measured (n = 8). (**E**) Serum TNF-α and IL-6 levels in mice were measured by ELISA (n = 8). (**F**) TNF-α and IL-6 mRNA levels in the pulmonary samples were determined using RT-qPCR analysis (n = 4). (**G**) Fibrosis-associated genes as shown were tested using RT-qPCR analysis (n = 4). (**H**) Genes associated with lung cancer progression were calculated using RT-qPCR analysis (n = 4). (**I**) IHC staining of c-Myc and SOX2 in pulmonary sections from the indicated groups of mice (n = 6). Scale bar, 100 μm. All data are expressed as mean ± SEM. *$^{*}p<0.05$* and *$^{**}p<0.01$* compared to the FA/IL-17a$^{+/+}$ group; *$^{+}p<0.05$* compared to the $PM_{2.5}$/IL-17a$^{+/+}$ group.

abolished in IL-17a$^{-/-}$ mice (Figure 8B). Markedly reduced total number of cells and the number of neutrophils in BALF were detected in IL-17a$^{-/-}$ mice following $PM_{2.5}$ exposure (Figure 8C, 8D). Compared to the $PM_{2.5}$/IL-17a$^{+/+}$ group, TNF-α and IL-6 expression levels in serum and lung tissues were markedly decreased in IL-17a$^{-/-}$ mice after $PM_{2.5}$ exposure for 3 months (Figure 8E, 8F). RT-qPCR analysis showed that IL-17a deletion evidently reduced the expression of MMP2, MMP9, TGF-β1, α-SMA, Fibronectin and Vimentin in pulmonary samples of $PM_{2.5}$-challenged mice compared to that of the wild type mice (Figure 8G). Furthermore, lung cancer markers including Kras, c-Myc, ABCG2, OCT4, SOX2 and Aldh1a1 induced by $PM_{2.5}$ were also markedly abolished when IL-17a was knocked out; however, p53 and PTEN mRNA expression levels restrained by $PM_{2.5}$ were significantly rescued in mice with the loss of IL-17a (Figure 8H). IHC staining confirmed the role of IL-17a$^{-/-}$ in suppressing c-Myc and SOX2 expression in lung tissues of $PM_{2.5}$-exposed mice (Figure 8I). The *in vivo* results above demonstrated that reducing IL-17a expression could alleviate $PM_{2.5}$-induced pulmonary injury and the expression of genes associated with lung cancer progression.

$PM_{2.5}$-promoted tumor growth and metastasis are associated with IL-17a in xenograft mouse models

In this regard, A549-drived xenograft mouse models were established using C57BL6 mice to further explore the effects of $PM_{2.5}$ on NSCLC progression, as well as the potential of IL-17a involved. As shown in Figure 9A–9C, the tumor size, volume and weight were highly promoted by $PM_{2.5}$ exposure compared to the Ctrl group, and similar results were observed in mice injected with IL-17a. Of note, $PM_{2.5}$-enhanced tumor growth was clearly abrogated in IL-17a$^{-/-}$ mice; however, this effect was restored when IL-17a was again injected to mice. In addition, no significant difference was observed in the change of body weight of mice from different groups (Figure 9D). KI-67, as a marker of cell proliferation, was clearly up-regulated by $PM_{2.5}$ exposure and IL-17a injection when compared to the Ctrl group. IL-17a deficiency considerably reduced KI-67 expression in tumor samples from $PM_{2.5}$-challenged mice, while being restored by IL-17a reinjection. Similar expression alterations were detected in SOX2 by IHC staining (Figure 9E). The *in vivo* metastasis was then investigated. Lung metastasis was greatly promoted in mice treated with $PM_{2.5}$ or IL-17a. Of note, compared to the wild type mice, IL-17a$^{-/-}$ mice exhibited markedly alleviated metastasis *in vivo* following $PM_{2.5}$ exposure, but this effect was abrogated when mice were re-injected with IL-17a (Figure 9F–9H). Finally, RT-qPCR results indicated that metastatic markers, including MMP2, MMP9, TGF-β1 and α-SMA, were markedly up-regulated by $PM_{2.5}$ exposure or IL-17a addition. Consistently, mice with IL-17a deficiency exhibited reduced expression of these genes, which were, however, significantly rescued by IL-17a reinjection to mice (Figure 9I). Collectively, these *in vivo* results illustrated that $PM_{2.5}$ exposure could accelerate the growth of NSCLC and metastasis, which was largely dependent on the expression of IL-17a.

DISCUSSION

NSCLC is a critical disease with high morbidity and mortality worldwide. Long-term $PM_{2.5}$ exposure is tightly associated with NSCLC progression. Increasing studies have shown the importance of IL-17a in promoting tumor development, including NSCLC, via multiple mechanisms [23–29]. In this research, chronic $PM_{2.5}$ exposure at high dose caused significant pulmonary damage and fibrosis. On the other, the expression levels of lung cancer biomarkers were highly induced by $PM_{2.5}$ exposure in lung tissues. IL-17a expression was markedly up-regulated in pulmonary samples, peripheral blood lymphocytes and splenic lymphocytes from $PM_{2.5}$-exposed mice. Clinical analysis demonstrated that IL-17a expression was significantly up-regulated in NSCLC patients. $PM_{2.5}$ exposure caused IL-17a expression in the isolated Th17 cells. Essentially, NSCLC cells cultured in the conditional medium from $PM_{2.5}$-incubated Th17 cells exhibited markedly increased cell proliferation and EMT processes. Consistently, recombinant human IL-17a considerably led to NSCLC cell proliferation, migration and invasion. Notably, the *in vivo* experiments further demonstrated that $PM_{2.5}$-induced pulmonary damage was alleviated in mice with IL-17a knockout. In addition, IL-17a deletion markedly abolished the role of $PM_{2.5}$ in promoting tumor growth and metastasis in mouse models. Taken together, all these results expanded the understanding of pulmonary carcinogenesis of $PM_{2.5}$ through increasing IL-17a expression levels, and thus IL-17a could be a biomarker for lung cancer prediction under the stress of $PM_{2.5}$.

Several molecular mechanisms contribute to the onset and pathogenesis of $PM_{2.5}$-induced lung injury, such as oxidative stress, inflammation and fibrosis [7–9]. In our present study, we further confirmed that $PM_{2.5}$ exposure led to significant inflammatory response in pulmonary tissues of mice, as evidenced by the significantly up-regulated expression of TNF-α and IL-6, which were in accordance with previous reports [8]. TGFβ1 is the most recognized isoform involved in respiratory diseases, which is important to the pro-fibrotic switch, matrix production, suppression of lung epithelial cells' proliferation, and is enhanced during pulmonary inflammation progress [42, 43]. TGFβ1 promotes the

expression of MMPs, including MMP2 and MMP9, and enhances the components of the extracellular matrix, such as collagens and fibronectins through up-regulating EMT-related transcription factors [32–34, 44]. A large number of studies have demonstrated the favorable effects of TGFβ1 on the pathological symptoms of lung injury, including $PM_{2.5}$-triggered pulmonary damage, which is associated with the extracellular matrix (ECM) accumulation and fibrosis formation [45, 46]. In our research, we also demonstrated that $PM_{2.5}$ exposure led to fibrosis in lung tissues, accompanied with significantly up-regulated expression of TGFβ1, MMP2, MMP9, Fibronectin, α-SMA and Vimentin.

Accumulating studies have indicated that TGFβ1 expression within the tumor microenvironment is frequently enhanced in NSCLC [47]. TGFβ1 stimulates tumor cell EMT, and promotes cell motility and

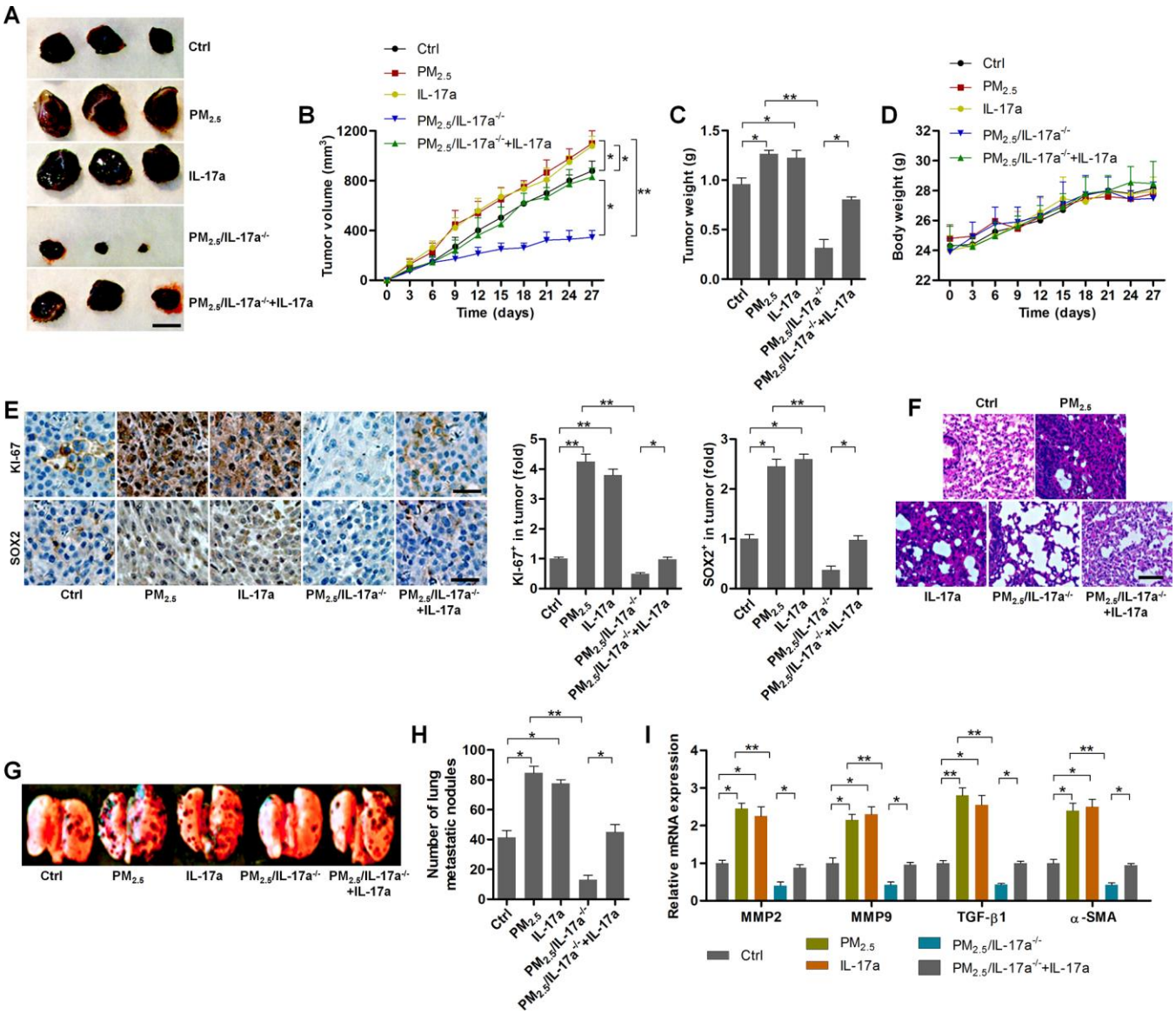

Figure 9. $PM_{2.5}$-promoted tumor growth and metastasis are associated with IL-17a in xenograft mouse models. (**A**) Representative images of tumor samples isolated from each group of mice as indicated (n = 6). Scale bar, 1 cm. (**B**) Tumor volume was measured (n = 6). (**C**) Tumor weight was recorded (n = 6). (**D**) The body weight of mice was recorded (n = 6). (**E**) IHC staining was used to determine KI-67 and SOX2 expression levels in the tumor sections (n = 4). Scale bar, 100 μm. (**F**) H&E staining of pulmonary tissues (n = 4; Scale bar, 100 μm) and (**G**) pictures of lung samples isolated from the indicated groups of mice to calculate the metastatic nodules on the surface of lungs (n = 6). (**H**) The number of lung metastatic nodules was quantified (n = 6). (**I**) RT-qPCR analysis was used to calculate the expression of metastasis-associated genes as displayed (n = 4). All data are expressed as mean ± SEM. *$p<0.05$ and **$p<0.01$.

metastasis via the activation of its down-streaming signaling pathways, subsequently favoring the expression of several transcriptional factors such as MMP2s, α-SMA and Fibronectin [48]. Therefore, TGF-β1 plays a critical role in inducing carcinogenesis. Previous studies have demonstrated that $PM_{2.5}$ exposure could enhance NSCLC progression, which was partly associated with the EMT event [17, 49]. Given the considerably activation of TGFβ1 signaling during lung cancer progression, we hypothesized that NSCLC might be also associated with the long-term $PM_{2.5}$ exposure. Herein, NSCLC biomarkers were measured in our study. RT-qPCR and IHC staining assays here demonstrated that the expression levels of lung cancer markers and cancer stem cell features of lung cells, including Kras, c-Myc, ABCG2, OCT4, SOX2 and Aldh1a1 [18, 36–38], were markedly increased in lung tissues of $PM_{2.5}$-challenged mice. In contrast, tumor suppressors p53 and PTEN [39] were decreased in pulmonary samples of mice in response to $PM_{2.5}$. All these *in vivo* findings validated that chronic $PM_{2.5}$ exposure enhanced the risk of lung cancer.

Th17 cells are enriched within peripheral blood mononuclear cells and tumor tissues. IL-17a is mainly produced by Th17 cells, which is closely associated with the development of various types of tumors, including lung cancer [26–28, 50]. Elevated IL-17-producing cells were involved in the poor survival and lymphangiogenesis in NSCLC patients [51]. In addition, IL-17 up-regulated the net angiogenic activity and the *in vivo* growth of NSCLC through increasing CXCR2-dependent angiogenesis [52]. Here in our study, the markedly increased expression of IL-17a was detected in lung tissues, peripheral blood lymphocytes and splenic lymphocytes of mice with long-term $PM_{2.5}$ exposure, further demonstrating the potential of $PM_{2.5}$ in inducing lung cancer by increasing IL-17a expression levels. The clinical analysis in our study showed that IL-17a expression was markedly up-regulated in NSCLC patients, and its elevation was associated with the worse overall survival rate, which was in line with previous study [51]. Increasing studies have illustrated that Th17/IL-17a axis may promote the progression of solid tumors (lung, liver and ovarian cancers) and hematologic cancers (chronic lymphocytic leukemia and myeloma) [31, 53–56]. Here, IL-17a expression was greatly increased by $PM_{2.5}$ in Th17 cells. NSCLC cells cultured in the conditional medium from $PM_{2.5}$-incubated Th17 cells showed significantly elevated cell proliferation and EMT process compared to the control group. Functions of IL-17 relevant to tumor involve the induction of cytokines such as IL-6 and TGF-β1 [57, 58]. Consistently, our *in vitro* findings indicated that IL-17a treatment evidently up-regulated TGF-β1 expression, as well as its down-streaming signals such as MMP2, MMP9, α-SMA, Fibronectin and Vimentin, implying the EMT event in NSCLC cells. These *in vitro* results revealed the critical role of IL-17a induced by $PM_{2.5}$ in promoting lung cancer development through accelerating EMT event. $PM_{2.5}$-challenged mice with IL-17a knockout exhibited markedly alleviated lung injury and cancer stem cell property. In addition, the *in vivo* subcutaneous tumor model confirmed that A549-drived tumor growth was further accelerated by $PM_{2.5}$, which was clearly abolished by the loss of IL-17a, accompanied with significantly reduced lung metastasis. Therefore, IL-17a might play a promotional role in $PM_{2.5}$-induced progression of lung cancer.

In conclusion, our study for the first time provided solid evidence that long-term $PM_{2.5}$ exposure could enhance the risk of NSCLC through promoting the expression of IL-17a, thereby increasing lung cancer cell proliferation and metastasis. Reducing IL-17a might be a promising strategy to treat air pollution-associated NSCLC. However, further studies are still warranted in future to investigate if there are other underlying mechanisms involved in $PM_{2.5}$-promoted lung cancer development.

MATERIALS AND METHODS

$PM_{2.5}$ sampling preparation

The procedures for $PM_{2.5}$ sampling preparation were referred to previous study with certain modification [59, 60]. In brief, to collect exposure mass, quartz filter (8 cm × 10 cm, 2500QAT-UP, Pallflex Products, Putnam, USA) was used to continuously and weekly collect $PM_{2.5}$ from Beijing Worker's Sports Complex located in the central area of Beijing (Beijing, China) from January 2017 to June 2017 at a flow rate of 180 L/min. All particle size we collected was less than 2.5 μm. Ambient $PM_{2.5}$ filters were stored at -80°C until experiments. The sampling was then treated with anhydrous alcohol and dissolved in pyrogen-free water. Subsequently, the extraction was sonicated for 2 days in an ultrasonic box and then concentrated through vacuum freeze-drying. Next, the double-distilled water was added to freeze-dried product, followed by centrifugation at 5000 rpm. The water-insoluble fraction was suspended in D-Hank's buffer (Gibco Corporation, USA) for further experiments. The organic content has been added in the supporting files (Supplementary Table 1).

Animals and treatments

Animal studies were performed in accordance with the principles of laboratory animal care (NIH publication revised 1985) and were approval by the Shandong Cancer Hospital and Institute, Shandong First Medical University and Shandong Academy of Medical Sciences

(Ji'nan, China). The wild type, male C57BL/6J (IL-17a$^{+/+}$) at 6-8 weeks of age were purchased from Beijing Vital River Laboratories (Beijing, China). The male IL-17a knockout (IL-17a$^{-/-}$) mice (with C57BL/6J background) also at 6-8 weeks of age were purchased from the Jackson Laboratory (Bar Harbor, ME). Prior to the animal experiments, all mice were allowed to acclimation for the lab condition for a week before PM exposure (animal numbers were listed in the figure legends). They were raised in a specific pathogen-free (SPF) facility at a controlled temperature and humidity (25 ± 2°C, 50 ± 5% humidity) environment with a standard 12 h/12 h light/dark cycle. All mice were given *ad libitum* access to water and food in their cages.

As for $PM_{2.5}$ challenge, IL-17a$^{+/+}$ and IL-17a$^{-/-}$ mice were exposed to either filtered air (FA) or $PM_{2.5}$ (168.5 ± 4.9 μg/m^3, flow rate of 80 L/min) for 6 h/day, 7 days/week for 1 week, 1 month or 3 months in an environmentally relevant and real-world PM with a PM-exposure system (Huironghe's Air Pollution Exposure System for the Whole Body of Animals, HAPES, Beijing Huironghe Technology Co. LTD., Beijing, China) to perform whole-body exposure of mice. The control (FA) mice were exposed to an identical protocol with the exception of a high-efficiency particulate-air filter positioned in the inlet valve to remove all of the $PM_{2.5}$ in the filtered air stream. After each treatment, all mice were sacrificed. Blood was collected from mice by cardiac puncture, and serum was centrifuged at 10,000 rpm for 10 min at 4°C. Then, the supernatant was collected for further analysis. The lung tissues were removed for histological, RT-qPCR and western blot analysis.

As for *in vivo* subcutaneous tumor model, the male C57BL/6 mice (8-10 weeks, IL-17a$^{+/+}$ and IL-17a$^{-/-}$) were used in the study. Hair in the lower dorsal skin of anesthetized mice was carefully trimmed with an electric clipper. A549 cells (1 × 10^6 cells/mouse) in 100 μL of PBS were subcutaneously injected in the hair-trimmed area on day 0. Then, all mice were randomly divided into 5 groups (animal numbers were listed in the figure legends), and treated as followings: 1) the IL-17a$^{+/+}$ Control (Ctrl) group without any treatments; 2) $PM_{2.5}$-exposed group of IL-17a$^{+/+}$ mice performed as described in the 4.2.1 section; 3) mice in the i.v. IL-17a group were injected with Recombinant Mouse IL-17a (1 μg/mouse per day; R&D System, USA) in sterile PBS intravenously through the tail vein; 4) $PM_{2.5}$-exposed group of IL-17a$^{-/-}$ mice also performed as described in the 4.21.1 section; 5) $PM_{2.5}$-exposed group of IL-17a$^{-/-}$ mice with the i.v. injection of Recombinant Mouse IL-17a (1 μg/mouse per day). During the treatments, the tumor size was measured every 2 days using calipers, and the body weight of mice was recorded. Tumor volume was calculated using the formula volume = (L × W^2) × 0.52, where L is the largest diameter and W is the smallest diameter. After treatments for 4 weeks, all mice were sacrificed and the tumors were dissected for weighing and further analysis.

For tumor metastasis assay, the A549 cells (1 × 10^6 cells/mouse) were implanted into IL-17a$^{+/+}$ or IL-17a$^{-/-}$ mice by tail vein injection. All mice were randomly divided into 5 groups (animal numbers were listed in the figure legends), and treated as followings: 1) the IL-17a$^{+/+}$ Control (Ctrl) group without any treatments; 2) $PM_{2.5}$-exposed group of IL-17a$^{+/+}$ mice performed as described in the 4.2.1 section; 3) mice in the i.v. IL-17a group were injected with Recombinant Mouse IL-17a (1 μg/mouse per day; R&D System) in sterile PBS intravenously through the tail vein; 4) $PM_{2.5}$-exposed group of IL-17a$^{-/-}$ mice also performed as described in the 4.21.1 section; 5) $PM_{2.5}$-exposed group of IL-17a$^{-/-}$ mice with the i.v. injection of Recombinant Mouse IL-17a (1 μg/mouse per day). Tumor metastasis was monitored. At 60 days after injection, all mice were sacrificed, the tumor nodules formed on the lung surfaces were analyzed, and the lung tissues were embedded in paraffin for H&E staining or stored for RT-qPCR analysis.

BALF isolation and analysis

BALF samples from each group of mice were simultaneously harvested. A total of 0.5 mL of BALF was collected. Then, total cells and neutrophils were counted using a hemocytometer in a double-blind manner for the calculation of the proportion of polymorphonuclear neutrophils. Protein concentrations in BALF were assessed using a BCA Protein Assay Kit (Pierce, USA) in accordance with the manufacturer's protocols.

ELISA assessments

TNF-α and IL-6 levels in serum (#ADI-900-047 for TNF-α, Peprotech, USA; #M6000B for IL-6, R&D System, USA) or supernatants (#DTA00D for TNF-α, R&D System; #D6050 for IL-6, R&D System) were measured using commercial kits according to the manufacturer's instructions. IL-17a contents in BALF, serum or supernatants of mice were measured using ELISA kit (BEK-2054-2P, Biosensis, Australia) purchased from Amyjet Scientific (Wuhan, China) following the protocols recommended by the manufacturer.

RT-qPCR

Total RNA was isolated from frozen lung tissues, tumor samples or the cultured cells using TRIZOL reagent

(Invitrogen, USA) following the manufacturer's instructions. Then, 2 μg of RNA was reverse-transcribed using the Transcriptor First Strand cDNA Synthesis Kit (Roche, USA). RT-qPCR assays were conducted by the use of the SYBR Premix Ex Taq II (TaKaRa, Dalian, China) on an ABI7900 real-time system (Applied Biosystems, USA). The PCR conditions were 95°C for 10 min; 40 cycles of 95°C for 10 s, 60°C for 10 s and 72°C for 20 s; and a final extension at 72°C for 10 min. The $2^{-\Delta\Delta Ct}$ method was used to quantify the relative expression level of RNA between groups. The transcription of the principal gene GAPDH was served as the internal control. The primer sequences for the genes used in the study were listed in Supplementary Table 2.

Western blotting

Proteins were extracted from lung tissues, tumor samples or cultured cells and homogenized in lysis buffer (Beyotime, Nanjing, China). The protein concentrations were calculated using a BCA Protein Assay Kit (Pierce) following the instructions provided by the manufacturer. Protein samples (20-50 μg) were separated on 8-12% SDS-PAGE gels and transferred to polyvinylidene difluoride (PVDF) membranes (Millipore, MA, USA). The membranes were then blocked using Tris-buffered saline containing Tween-20 (TBST) with 5% skim milk powder for 1.5 h at room temperature, followed by incubation with primary antibodies (IL-17a, PA5-46947, ThermoFisher Scientific, USA; GAPDH, ab8245, Abcam) overnight at 4°C. Then, the membranes were incubated with a horseradish peroxidase (HRP)-conjugated anti-mouse or anti-rabbit IgG antibody (Abcam) for 1 h at room temperature. Membranes were finally treated with ECL reagents (Millipore) according to the manufacturer's instructions. GAPDH was served as the loading control.

Immunohistochemistry analysis

The pulmonary tissues or tumor samples were isolated from each group of mice as indicated, immersed in 4% paraformaldehyde for 24 h and then transferred to 70% ethanol. After dehydrated, all tissue samples were embedded in paraffin, and sectioned at 5-μm thickness. Then, the sections were stained with hematoxylin and eosin (H&E) or Masson's trichrome kit (Nanjing Jiancheng Co., Ltd., Nanjing, China) according to the manufacturers' protocols. Immunohistochemistry (IHC) was performed using the streptavidin peroxidase (SP, Jackson ImmunoResearch Inc., USA) method according to the kit's protocols. The obtained tissue sections were then immersed in sodium citrate, heated in water-bath for 10 min at 98°C for antigen retrieval, and cooled to room temperature. Next, endogenous peroxidase was blocked using 3% hydrogen peroxide for 10 min. After washing with PBS, the tissue sections were treated with 5% normal goat serum (KeyGen Biotech, Nanjing, China), and then were incubated with the primary antibodies against c-Myc (ab32072, Abcam), OCT4 (ab18976, Abcam), SOX2 (PA1-094, ThermoFisher Scientific), IL-17a (ab79056, Abcam), IL-17a (PA5-79470, ThermoFisher Scientific) and KI-67 (MA5-14520, ThermoFisher Scientific) overnight at 4°C. Then, horseradish peroxidase (HRP)-conjugated secondary antibodies (Abcam) were used to visualize the antibody signal with diaminobenzidine (DAB, KeyGen Biotech). The tissue sections were calculated under a light microscope (Nikon, Japan). The quantification of IHC results was performed using Image-Pro Plus 6.0 software (Media Cybernetics, USA).

Human samples

48 pairs of fresh lung cancer and the adjacent noncancerous tissues were collected from the Shandong Cancer Hospital and Institute, Shandong First Medical University and Shandong Academy of Medical Sciences (Ji'nan, China). The clinic pathological characteristics of patients were shown in Supplementary Table 3. These clinical tissue samples were histologically confirmed by H&E staining. The study was approved by the Ethics Committee of the Shandong Cancer Hospital and Institute, Shandong First Medical University and Shandong Academy of Medical Sciences, and was conducted in accordance with the ethical principles indicted by the Helsinki Declaration. The informed consent was obtained from all patients involved.

Cells and culture

Lymphocyte isolation from spleen

The spleen samples were isolated from each group of mice following $PM_{2.5}$ challenge or not, and washed with PBS. Then, the spleen tissues were placed in a 200-mesh stain steel sieve over a culture dish supplemented with 5 mL lymphocyte isolation separation medium (Absin, Shanghai, China) and grounded into small pieces using the plunger of glass syringe. Then, the liquid was transferred into a centrifuge tube, and 200-500 μL of RPMI-1640 medium (Gibco) was added to the tube, followed by centrifugation at 800 × g for 30 min at room temperature. After centrifugation, three layers were formed. The middle milky layer containing lymphocytes was subsequently transferred into a new test tube. The obtained lymphocytes were rinsed with PBS, suspended in RPMI-1640 medium (Gibco) with 10 % fetal calf serum (Solarbio), and then transferred into a culture bottle. All these procedures were performed under sterile condition. Finally, the lympho-

cyte viability was measured following the trypan blue exclusion criteria, and the viability was over 95%. The purified lymphocyte was finally used for ELISA analysis.

Peripheral blood mononuclear cells (PBMCs) isolation

PBMCs were isolated from mouse peripheral blood samples using the standard Ficoll-Hypaque density gradient centrifugation methods as previously indicated [61, 62]. In brief, T lymphocytes were prepared from mouse PBMCs by negative selection with magnetic bead depletion of non-T lymphocytes with the EasySep mouse T lymphocytes isolation kit (Stemcell Technologies, USA) according to the instructions provided by the manufacturer. Then, the purity of T lymphocytes was calculated using the flow cytometry analysis and was found to be greater than 95%.

Th17 differentiation, NSCLC cell culture and treatment

At first, total splenic T cells were purified using the negative selection with the EasySep™ Mouse $CD4^+$ T Cell Isolation Kit (Stemcell Technologies, Canada) according to the manufacturer's protocols, and then were purified to > 95%. $CD4^+$ purity was assessed through FACS-sorting using anti-CD4 FITC (Becton Dickinson, USA). For gating, viable cells were selected according to their Forward-scatter (FSC) values. Next, T-helper cells were isolated as $CD4^+$ cells (> 97% total viable cells). T cells were planted in 12-well plates supplemented with plate bound 5 μg/ml of anti-CD3 (Abcam) and 2 μg/ml of soluble anti-CD28 (Abcam) antibodies at 2×10^6 cells/well in RPMI 1640 medium (Gibco) containing 15% inactivated fetal bovine serum (FBS, Gibco). For Th17 cell differentiation, splenic T cells were incubated with IL-6 (20 ng/ml), IL-23 (15 ng/ml), IL-1β (10 ng/ml), and TGF-β (5 ng/ml) (all from Invitrogen, USA), and IFN-γ-IL-2- and IL-4 directed antibodies (R&D Systems) as previously indicated [63]. Th17 differentiation was measured using flow cytometry [64]. Then, $PM_{2.5}$ at 100 μg/cm^2 was subjected to the obtained Th17 cells for 24 h. The supernatants and cells after treatments were collected for ELISA, RT-qPCR, western blot and IF assays.

Human NSCLC cells including A549 and H1350 were purchased from the American Type Culture Collection (ATCC, Manassas, USA). All these cancer cells were grown in RPMI 1640 medium (Gibco, USA) supplemented with 10% FBS (Gibco) and 100 U/mL penicillin/streptomycin. Cells were grown at 37°C in a humidified atmosphere containing 5% CO_2 and 95% air. Recombinant human IL-17a (R&D System) was used to stimulate NSCLC cells as described in the figure legends.

CCK-8 analysis and EdU determination

After each treatment, the cell viability analysis was conducted using the CCK-8 detection kit (Dojindo, Kumamoto, Japan) according to the protocols as described by the manufacturer. Finally, the absorbance was measured with a microplate reader at a wavelength of 450 nm.

After treatments, the cell proliferation ability was calculated through the EdU incorporation assay with the EdU Assay Kits (Life Technologies, USA) following the protocols recommended by the manufacturer, and was finally observed with a fluorescent microscope (Olympus, Japan).

Colony formation analysis

For colony formation analysis, 1000 cells after treatments were plated in a 10 cm dish and allowed to grow for 14 days at 37°C in 5% CO_2. Then, the surviving colonies (more than 50 cells in each colony) were counted using a microscope following Giemsa staining.

Immunofluorescence (IF) staining

After treatments, the cells were fixed in 4% paraformaldehyde for 20 min and permeated using 0.5% Triton X-100 (Solarbio, Beijing, China) in PBS for 5 min. After blocking with 5% goat serum (Solarbio) for 1 h, the cells were incubated with primary antibodies (anti-IL-17a antibody, Abcam, ab79056; anti-N-cadherin antibody, Abcam, ab18203) at 1:100 dilutions overnight at 4°C in a humidified chamber, followed by incubation with fluorescently labeled secondary antibodies (goat anti-rabbit IgG H&L, Abcam, ab150077; goat anti-rabbit IgG H&L, Abcam, ab150088) for 1 h. Then, the cells were counterstained with DAPI (Beyotime) for nuclear staining. The images were observed under a fluorescence microscope (Olympus), and the images were analyzed using Image Pro Plus 6.0.

Transwell analysis

For the migration analysis, the treated cells were suspended in serum-free DMEM (Gibco), and 1×10^5 cells were then plated in the top chamber lined with an uncoated 8.0 μm pore membrane (Millipore). For the invasion analysis, 1×10^5 cells were plated in the top chamber coated with Matrigel (Corning, USA). Subsequently, the chambers were inserted into a 24-well plate supplemented with DMEM containing 20% FBS (Gibco). After incubation for 24 h at 37°C in 5% CO_2, the cells undergoing migration or invasion through the membrane were stained using 0.1% crystal violet, and were quantified with a microscope (Olympus).

Wound healing assays

Cell motility was calculated through the use of a scratch wound assay. The cells and the controls were incubated in 6-well dishes with or without the conditional medium until 80-90% confluent. Then, the cell layers were carefully wounded with sterile tips and washed twice with fresh medium. Cells were incubated with fresh medium and observed under a microscope at 24 h after wounding. Three random visual fields were quantified.

Statistical analysis

Data in our study were represented as Means ± standard error of the mean (SEM). Differences among groups were analyzed using one-way analysis of variance (ANOVA), followed by a post hoc Tukey's test. Comparisons between two groups were performed using an unpaired Student's t-test. The survival rate was analyzed using the Kaplan-Meier method. All results were analyzed using GraphPad Prism Software Version 6.0 (GraphPad Software, California, USA). Differences were considered to be significant when p value < 0.05. All experimenters were blinded to the animal genotype and grouping information. Data from the animal experiments were collected through a blinded manner. All *in vitro* experiments were repeated at least three independent times unless specifically demonstrated in the figure legends.

CONFLICTS OF INTEREST

The authors declare no conflicts of interest.

REFERENCES

1. Li N, Hao M, Phalen RF, Hinds WC, Nel AE. Particulate air pollutants and asthma. A paradigm for the role of oxidative stress in PM-induced adverse health effects. Clin Immunol. 2003; 109:250–65. https://doi.org/10.1016/j.clim.2003.08.006 PMID:14697739

2. Lim SS, Vos T, Flaxman AD, Danaei G, Shibuya K, Adair-Rohani H, Amann M, Anderson HR, Andrews KG, Aryee M, Atkinson C, Bacchus LJ, Bahalim AN, et al. A comparative risk assessment of burden of disease and injury attributable to 67 risk factors and risk factor clusters in 21 regions, 1990-2010: a systematic analysis for the global burden of disease study 2010. Lancet. 2012; 380:2224–60. https://doi.org/10.1016/S0140-6736(12)61766-8 PMID:23245609

3. Xu MX, Ge CX, Qin YT, Gu TT, Lou DS, Li Q, Hu LF, Feng J, Huang P, Tan J. Prolonged PM2.5 exposure elevates risk of oxidative stress-driven nonalcoholic fatty liver disease by triggering increase of dyslipidemia. Free Radic Biol Med. 2019; 130:542–56. https://doi.org/10.1016/j.freeradbiomed.2018.11.016 PMID:30465824

4. Pope CA 3rd, Burnett RT, Thun MJ, Calle EE, Krewski D, Ito K, Thurston GD. Lung cancer, cardiopulmonary mortality, and long-term exposure to fine particulate air pollution. JAMA. 2002; 287:1132–41. https://doi.org/10.1001/jama.287.9.1132 PMID:11879110

5. Xing YF, Xu YH, Shi MH, Lian YX. The impact of PM2.5 on the human respiratory system. J Thorac Dis. 2016; 8:E69–74. https://doi.org/10.3978/j.issn.2072-1439.2016.01.19 PMID:26904255

6. Turner MC, Krewski D, Pope CA 3rd, Chen Y, Gapstur SM, Thun MJ. Long-term ambient fine particulate matter air pollution and lung cancer in a large cohort of never-smokers. Am J Respir Crit Care Med. 2011; 184:1374–81. https://doi.org/10.1164/rccm.201106-1011OC PMID:21980033

7. Weichenthal SA, Godri-Pollitt K, Villeneuve PJ. PM2.5, oxidant defence and cardiorespiratory health: a review. Environ Health. 2013; 12:40. https://doi.org/10.1186/1476-069X-12-40 PMID:23641908

8. Riva DR, Magalhães CB, Lopes AA, Lanças T, Mauad T, Malm O, Valença SS, Saldiva PH, Faffe DS, Zin WA. Low dose of fine particulate matter (PM2.5) can induce acute oxidative stress, inflammation and pulmonary impairment in healthy mice. Inhal Toxicol. 2011; 23:257–67. https://doi.org/10.3109/08958378.2011.566290 PMID:21506876

9. Dagher Z, Garçon G, Billet S, Gosset P, Ledoux F, Courcot D, Aboukais A, Shirali P. Activation of different pathways of apoptosis by air pollution particulate matter (PM2.5) in human epithelial lung cells (L132) in culture. Toxicology. 2006; 225:12–24. https://doi.org/10.1016/j.tox.2006.04.038 PMID:16787692

10. Vinikoor-Imler LC, Davis JA, Luben TJ. An ecologic analysis of county-level PM2.5 concentrations and lung cancer incidence and mortality. Int J Environ Res Public Health. 2011; 8:1865–71. https://doi.org/10.3390/ijerph8061865 PMID:21776206

11. Fu J, Jiang D, Lin G, Liu K, Wang Q. An ecological analysis of PM2.5 concentrations and lung cancer mortality rates in China. BMJ Open. 2015; 5:e009452. https://doi.org/10.1136/bmjopen-2015-009452 PMID:26603253

12. Hirsch FR, Scagliotti GV, Mulshine JL, Kwon R, Curran WJ Jr, Wu YL, Paz-Ares L. Lung cancer: current therapies and new targeted treatments. Lancet. 2017; 389:299–311. https://doi.org/10.1016/S0140-6736(16)30958-8 PMID:27574741

13. Manchado E, Weissmueller S, Morris JP 4th, Chen CC, Wullenkord R, Lujambio A, de Stanchina E, Poirier JT, Gainor JF, Corcoran RB, Engelman JA, Rudin CM, Rosen N, Lowe SW. A combinatorial strategy for treating KRAS-mutant lung cancer. Nature. 2016; 534:647–51. https://doi.org/10.1038/nature18600 PMID:27338794

14. Jamal-Hanjani M, Wilson GA, McGranahan N, Birkbak NJ, Watkins TB, Veeriah S, Shafi S, Johnson DH, Mitter R, Rosenthal R, Salm M, Horswell S, Escudero M, et al, and TRACERx Consortium. Tracking the evolution of non-small-cell lung cancer. N Engl J Med. 2017; 376:2109–21. https://doi.org/10.1056/NEJMoa1616288 PMID:28445112

15. Bilfinger T, Keresztes R, Albano D, Nemesure B. Five-year survival among stage IIIA lung cancer patients receiving two different treatment modalities. Med Sci Monit. 2016; 22:2589–94. https://doi.org/10.12659/msm.898675 PMID:27442604

16. David EA, Clark JM, Cooke DT, Melnikow J, Kelly K, Canter RJ. The role of thoracic surgery in the therapeutic management of metastatic non-small cell lung cancer. J Thorac Oncol. 2017; 12:1636–45. https://doi.org/10.1016/j.jtho.2017.08.008 PMID:28843357

17. Deng X, Feng N, Zheng M, Ye X, Lin H, Yu X, Gan Z, Fang Z, Zhang H, Gao M, Zheng ZJ, Yu H, Ding W, Qian B. PM2.5 exposure-induced autophagy is mediated by lncRNA loc146880 which also promotes the migration and invasion of lung cancer cells. Biochim Biophys Acta Gen Subj. 2017; 1861:112–25. https://doi.org/10.1016/j.bbagen.2016.11.009 PMID:27836757

18. Wei H, Liang F, Cheng W, Zhou R, Wu X, Feng Y, Wang Y. The mechanisms for lung cancer risk of $PM_{2.5}$: induction of epithelial-mesenchymal transition and cancer stem cell properties in human non-small cell lung cancer cells. Environ Toxicol. 2017; 32:2341–51. https://doi.org/10.1002/tox.22437 PMID:28846189

19. Wang Y, Zhong Y, Hou T, Liao J, Zhang C, Sun C, Wang G. PM2.5 induces EMT and promotes CSC properties by activating notch pathway in vivo and vitro. Ecotoxicol Environ Saf. 2019; 178:159–67. https://doi.org/10.1016/j.ecoenv.2019.03.086 PMID:31002970

20. Beringer A, Noack M, Miossec P. IL-17 in chronic inflammation: from discovery to targeting. Trends Mol Med. 2016; 22:230–41. https://doi.org/10.1016/j.molmed.2016.01.001 PMID:26837266

21. Eyerich K, Dimartino V, Cavani A. IL-17 and IL-22 in immunity: driving protection and pathology. Eur J Immunol. 2017; 47:607–14. https://doi.org/10.1002/eji.201646723 PMID:28295238

22. Son HJ, Lee SH, Lee SY, Kim EK, Yang EJ, Kim JK, Seo HB, Park SH, Cho ML. Oncostatin M suppresses activation of IL-17/Th17 via SOCS3 regulation in CD4+ T cells. J Immunol. 2017; 198:1484–91. https://doi.org/10.4049/jimmunol.1502314 PMID:28093521

23. González-Amaro R, Marazuela M. T regulatory (treg) and T helper 17 (Th17) lymphocytes in thyroid autoimmunity. Endocrine. 2016; 52:30–38. https://doi.org/10.1007/s12020-015-0759-7 PMID:26475497

24. Kuai DY, Cheng J, Yang RC, Liu T, Liu H, Liu FG, Gao CX, Xin S, Li J, Zhu ST, Zhang ST, Xu BH. Th17/Treg cell imbalance in patients with early esophageal squamous cell carcinoma. International Journal of Clinical and Experimental Pathology. 2016; 9:8485–91.

25. Amicarella F, Muraro MG, Hirt C, Cremonesi E, Padovan E, Mele V, Governa V, Han J, Huber X, Droeser RA, Zuber M, Adamina M, Bolli M, et al. Dual role of tumour-infiltrating T helper 17 cells in human colorectal cancer. Gut. 2017; 66:692–704. https://doi.org/10.1136/gutjnl-2015-310016 PMID:26719303

26. Zhao C, Li Y, Zhang W, Zhao D, Ma L, Ma P, Yang F, Wang Y, Shu Y, Qiu W. IL-17 induces NSCLC A549 cell proliferation via the upregulation of HMGA1, resulting in an increased cyclin D1 expression. Int J Oncol. 2018; 52:1579–92. https://doi.org/10.3892/ijo.2018.4307 PMID:29512693

27. Kirshberg S, Izhar U, Amir G, Demma J, Vernea F, Beider K, Shlomai Z, Wald H, Zamir G, Shapira OM, Peled A, Wald O. Involvement of CCR6/CCL20/IL-17 axis in NSCLC disease progression. PLoS One. 2011; 6:e24856. https://doi.org/10.1371/journal.pone.0024856 PMID:21949768

28. Li Q, Han Y, Fei G, Guo Z, Ren T, Liu Z. IL-17 promoted metastasis of non-small-cell lung cancer cells. Immunol Lett. 2012; 148:144–50. https://doi.org/10.1016/j.imlet.2012.10.011 PMID:23089548

29. Pappu R, Ramirez-Carrozzi V, Ota N, Ouyang W, Hu Y. The IL-17 family cytokines in immunity and disease. J Clin Immunol. 2010; 30:185–95. https://doi.org/10.1007/s10875-010-9369-6 PMID:20177959

30. Gu C, Wu L, Li X. IL-17 family: cytokines, receptors and signaling. Cytokine. 2013; 64:477–85. https://doi.org/10.1016/j.cyto.2013.07.022 PMID:24011563

31. Reppert S, Koch S, Finotto S. IL-17A is a central regulator of lung tumor growth. Oncoimmunology. 2012; 1:783–85. https://doi.org/10.4161/onci.19735 PMID:22934282

32. Kage H, Borok Z. EMT and interstitial lung disease: a mysterious relationship. Curr Opin Pulm Med. 2012; 18:517–23. https://doi.org/10.1097/MCP.0b013e3283566721 PMID:22854509

33. Borthwick LA, Gardner A, De Soyza A, Mann DA, Fisher AJ. Transforming growth factor-β1 (TGF-β1) driven epithelial to mesenchymal transition (EMT) is accentuated by tumour necrosis factor α (TNFα) via crosstalk between the SMAD and NF-κB pathways. Cancer Microenviron. 2012; 5:45–57. https://doi.org/10.1007/s12307-011-0080-9 PMID:21792635

34. Câmara J, Jarai G. Epithelial-mesenchymal transition in primary human bronchial epithelial cells is smad-dependent and enhanced by fibronectin and TNF-alpha. Fibrogenesis Tissue Repair. 2010; 3:2. https://doi.org/10.1186/1755-1536-3-2 PMID:20051102

35. Rokavec M, Öner MG, Li H, Jackstadt R, Jiang L, Lodygin D, Kaller M, Horst D, Ziegler PK, Schwitalla S, Slotta-Huspenina J, Bader FG, Greten FR, Hermeking H. IL-6R/STAT3/miR-34a feedback loop promotes EMT-mediated colorectal cancer invasion and metastasis. J Clin Invest. 2014; 124:1853–67. https://doi.org/10.1172/JCI73531 PMID:24642471

36. Shankar S, Nall D, Tang SN, Meeker D, Passarini J, Sharma J, Srivastava RK. Resveratrol inhibits pancreatic cancer stem cell characteristics in human and KrasG12D transgenic mice by inhibiting pluripotency maintaining factors and epithelial-mesenchymal transition. PLoS One. 2011; 6:e16530. https://doi.org/10.1371/journal.pone.0016530 PMID:21304978

37. Fujiki H, Sueoka E, Rawangkan A, Suganuma M. Human cancer stem cells are a target for cancer prevention using (-)-epigallocatechin gallate. J Cancer Res Clin Oncol. 2017; 143:2401–12. https://doi.org/10.1007/s00432-017-2515-2 PMID:28942499

38. Martins-Neves SR, Cleton-Jansen AM, Gomes CM. Therapy-induced enrichment of cancer stem-like cells in solid human tumors: where do we stand? Pharmacol Res. 2018; 137:193–204. https://doi.org/10.1016/j.phrs.2018.10.011 PMID:30316903

39. Zheng H, Ying H, Yan H, Kimmelman AC, Hiller DJ, Chen AJ, Perry SR, Tonon G, Chu GC, Ding Z, Stommel JM, Dunn KL, Wiedemeyer R, et al. P53 and pten control neural and glioma stem/progenitor cell renewal and differentiation. Nature. 2008; 455:1129–33. https://doi.org/10.1038/nature07443 PMID:18948956

40. Ahn SH, Edwards AK, Singh SS, Young SL, Lessey BA, Tayade C. IL-17A contributes to the pathogenesis of endometriosis by triggering proinflammatory cytokines and angiogenic growth factors. J Immunol. 2015; 195:2591–600. https://doi.org/10.4049/jimmunol.1501138 PMID:26259585

41. Wang H, Li M, Zhang R, Wang Y, Zang W, Ma Y, Zhao G, Zhang G. Effect of miR-335 upregulation on the apoptosis and invasion of lung cancer cell A549 and H1299. Tumour Biol. 2013; 34:3101–09. https://doi.org/10.1007/s13277-013-0878-9 PMID:23740614

42. Györfi AH, Matei AE, Distler JH. Targeting TGF-β signaling for the treatment of fibrosis. Matrix Biol. 2018; 68:8–27. https://doi.org/10.1016/j.matbio.2017.12.016 PMID:29355590

43. Weng D, Chen JX, Li HH, Liu F, Zhou LD, Liu HP, Zheng RJ, Jiang Y, Liu ZH, Ge B. 2-aminopurine suppresses the TGF-β1-induced epithelial-mesenchymal transition and attenuates bleomycin-induced pulmonary fibrosis. Cell Death Discov. 2018; 4:17. https://doi.org/10.1038/s41420-017-0016-3 PMID:29531814

44. Willis BC, duBois RM, Borok Z. Epithelial origin of myofibroblasts during fibrosis in the lung. Proc Am Thorac Soc. 2006; 3:377–82. https://doi.org/10.1513/pats.200601-004TK PMID:16738204

45. Gu LZ, Sun H, Chen JH. Histone deacetylases 3 deletion restrains PM2.5-induced mice lung injury by regulating NF-κB and TGF-β/Smad2/3 signaling pathways. Biomed Pharmacother. 2017; 85:756–62. https://doi.org/10.1016/j.biopha.2016.11.094 PMID:27919737

46. Zhang H, Xue L, Li B, Tian H, Zhang Z, Tao S. Therapeutic potential of bixin in PM2.5 particles-

induced lung injury in an Nrf2-dependent manner. Free Radic Biol Med. 2018; 126:166–76. https://doi.org/10.1016/j.freeradbiomed.2018.08.015 PMID:30120979

47. Wang J, Qiao XY, Lu FH, Zhou ZG, Song YZ, Huo JJ, Liu X. TGF-beta1 in serum and induced sputum for predicting radiation pneumonitis in patients with non-small cell lung cancer after radiotherapy. Chin J Cancer. 2010; 29:325–29. https://doi.org/10.5732/cjc.009.10454 PMID:20193119

48. Ko H, So Y, Jeon H, Jeong MH, Choi HK, Ryu SH, Lee SW, Yoon HG, Choi KC. TGF-β1-induced epithelial-mesenchymal transition and acetylation of Smad2 and Smad3 are negatively regulated by EGCG in human A549 lung cancer cells. Cancer Lett. 2013; 335:205–13. https://doi.org/10.1016/j.canlet.2013.02.018 PMID:23419524

49. Yang D, Ma M, Zhou W, Yang B, Xiao C. Inhibition of miR-32 activity promoted EMT induced by PM2.5 exposure through the modulation of the Smad1-mediated signaling pathways in lung cancer cells. Chemosphere. 2017; 184:289–98. https://doi.org/10.1016/j.chemosphere.2017.05.152 PMID:28601662

50. Benevides L, Cardoso CR, Tiezzi DG, Marana HR, Andrade JM, Silva JS. Enrichment of regulatory T cells in invasive breast tumor correlates with the upregulation of IL-17A expression and invasiveness of the tumor. Eur J Immunol. 2013; 43:1518–28. https://doi.org/10.1002/eji.201242951 PMID:23529839

51. Chen X, Xie Q, Cheng X, Diao X, Cheng Y, Liu J, Xie W, Chen Z, Zhu B. Role of interleukin-17 in lymphangiogenesis in non-small-cell lung cancer: enhanced production of vascular endothelial growth factor C in non-small-cell lung carcinoma cells. Cancer Sci. 2010; 101:2384–90. https://doi.org/10.1111/j.1349-7006.2010.01684.x PMID:20825419

52. Numasaki M, Watanabe M, Suzuki T, Takahashi H, Nakamura A, McAllister F, Hishinuma T, Goto J, Lotze MT, Kolls JK, Sasaki H. IL-17 enhances the net angiogenic activity and in vivo growth of human non-small cell lung cancer in SCID mice through promoting CXCR-2-dependent angiogenesis. J Immunol. 2005; 175:6177–89. https://doi.org/10.4049/jimmunol.175.9.6177 PMID:16237115

53. Gomes AL, Teijeiro A, Burén S, Tummala KS, Yilmaz M, Waisman A, Theurillat JP, Perna C, Djouder N. Metabolic inflammation-associated IL-17A causes non-alcoholic steatohepatitis and hepatocellular carcinoma. Cancer Cell. 2016; 30:161–75. https://doi.org/10.1016/j.ccell.2016.05.020 PMID:27411590

54. Charles KA, Kulbe H, Soper R, Escorcio-Correia M, Lawrence T, Schultheis A, Chakravarty P, Thompson RG, Kollias G, Smyth JF, Balkwill FR, Hagemann T. The tumor-promoting actions of TNF-alpha involve TNFR1 and IL-17 in ovarian cancer in mice and humans. J Clin Invest. 2009; 119:3011–23. https://doi.org/10.1172/JCI39065 PMID:19741298

55. Hus I, Bojarska-Junak A, Chocholska S, Tomczak W, Woś J, Dmoszyńska A, Roliński J. Th17/IL-17A might play a protective role in chronic lymphocytic leukemia immunity. PLoS One. 2013; 8:e78091. https://doi.org/10.1371/journal.pone.0078091 PMID:24223764

56. Prabhala RH, Fulciniti M, Pelluru D, Rashid N, Nigroiu A, Nanjappa P, Pai C, Lee S, Prabhala NS, Bandi RL, Smith R, Lazo-Kallanian SB, Valet S, et al. Targeting IL-17A in multiple myeloma: a potential novel therapeutic approach in myeloma. Leukemia. 2016; 30:379–89. https://doi.org/10.1038/leu.2015.228 PMID:26293646

57. Wainwright DA, Sengupta S, Han Y, Ulasov IV, Lesniak MS. The presence of IL-17A and T helper 17 cells in experimental mouse brain tumors and human glioma. PLoS One. 2010; 5:e15390. https://doi.org/10.1371/journal.pone.0015390 PMID:21060663

58. Novitskiy SV, Pickup MW, Gorska AE, Owens P, Chytil A, Aakre M, Wu H, Shyr Y, Moses HL. TGF-β receptor II loss promotes mammary carcinoma progression by Th17 dependent mechanisms. Cancer Discov. 2011; 1:430–41. https://doi.org/10.1158/2159-8290.CD-11-0100 PMID:22408746

59. Ying Z, Xu X, Bai Y, Zhong J, Chen M, Liang Y, Zhao J, Liu D, Morishita M, Sun Q, Spino C, Brook RD, Harkema JR, Rajagopalan S. Long-term exposure to concentrated ambient PM2.5 increases mouse blood pressure through abnormal activation of the sympathetic nervous system: a role for hypothalamic inflammation. Environ Health Perspect. 2014; 122:79–86. https://doi.org/10.1289/ehp.1307151 PMID:24240275

60. Ogino K, Zhang R, Takahashi H, Takemoto K, Kubo M, Murakami I, Wang DH, Fujikura Y. Allergic airway inflammation by nasal inoculation of particulate matter (PM2.5) in NC/nga mice. PLoS One. 2014; 9:e92710. https://doi.org/10.1371/journal.pone.0092710 PMID:24671176

61. Kashiyama N, Miyagawa S, Fukushima S, Kawamura T, Kawamura A, Yoshida S, Nakamura Y, Harada A,

Masuda H, Toda K, Asahara T, Sawa Y. Vasculogenically conditioned peripheral blood mononuclear cells inhibit mouse immune response to induced pluripotent stem cell-derived allogeneic cardiac grafts. PLoS One. 2019; 14:e0217076. https://doi.org/10.1371/journal.pone.0217076 PMID:31136599

62. Zhang R, Wang X, Hong M, Luo T, Zhao M, Shen H, Fang J, Li X, Zang S, Chen P, Nie D, Zheng P, Wu Q, Xia L. Endothelial microparticles delivering microRNA-155 into T lymphocytes are involved in the initiation of acute graft-versus-host disease following allogeneic hematopoietic stem cell transplantation. Oncotarget. 2017; 8:23360–75. https://doi.org/10.18632/oncotarget.15579 PMID:28423578

63. Zhou Z, Sun W, Liang Y, Gao Y, Kong W, Guan Y, Feng J, Wang X. Fenofibrate inhibited the differentiation of T helper 17 cells in vitro. PPAR Res. 2012; 2012:145654. https://doi.org/10.1155/2012/145654 PMID:22792085

64. Li B, Wang X, Choi IY, Wang YC, Liu S, Pham AT, Moon H, Smith DJ, Rao DS, Boldin MP, Yang L. miR-146a modulates autoreactive Th17 cell differentiation and regulates organ-specific autoimmunity. J Clin Invest. 2017; 127:3702–16. https://doi.org/10.1172/JCI94012 PMID:28872459

SUPPLEMENTARY MATERIALS

Supplementary Tables

Supplementary Table 1. Components of the collected $PM_{2.5}$ (ng/m^3) used in the study.

Element	Ambient $PM_{2.5}$
Magnesium	26.75 ± 3.96
Selenium	0.46 ±0.04
Cerium	0.04 ± 0.01
Copper	2.96 ± 0.32
Potassium	36.74 ± 7.58
Barium	3.29 ± 0.18
Sodium	59.07 ± 8.23
Lead	2.08 ± 0.96
Sulfur	1036.72 ± 378.29
Aluminum	28.63 ± 8.47
Cadmium	0.53 ± 0.07
Strontium	0.48 ± 0.18
Rubidium	0.08 ± 0.02
Nitrogen	0.39 ± 0.28
Cobalt	0.11 ±0.01
Iron	59.25 ± 11.29
Lanthanum	0.02 ± 0.01
Manganese	1.72 ± 0.47
Antimony	0.52 ± 0.29
Molybdenum	0.74 ± 0.20
Chromium	7.19 ± 1.08
Vanadium	0.36 ± 0.14
Phosphorus	17.07 ± 3.08
Arsenic	0.92 ± 0.18
Titanium	0.97 ± 0.05
Calcium	93.53 ± 14.09
Zinc	10.96 ± 1.68

Supplementary Table 2. The primer sequences for the genes used in the study.

Primers	Forward Sequence (5'-3')	Reverse Sequence (5'-3')
mMMP2	TTCCGCTTCCAGGGCACA	CACCTTCTGAGTTCCCACCAA
mTNF-α	ACCTGGCCTCTCTACCTTGT	CCCGTAGGGCGATTACAGTC
mIL-6	CAACGATGATGCACTTGCAGA	TCTCTCTGAAGGACTCTGGCT
mMMP9	CGTCGTGATCCCCACTTACT	CGTCGTGATCCCCACTTACT
mTGF-β1	GACTCTCCACCTGCAAGACC	GACTCTCCACCTGCAAGACC
mα-SMA	CTGCCGAGCGTGAGATTGT	CTTCGTCGTATTCCTGTTTGCT
mFibronectin	CATGAAGGGGGTCAGTCCTA	TAGGTTTGCAGGTCCATTCC
mVimentin	TGGACGTTTCCAAGCCTGAC	CTGTCTCCGGTACTCGTTTGACT
mKras	AGACACGAAACAGGCTCAGG	GCATCGTCAACACCCTGTCT
mc-Myc	TCACCAGCACAACTACGCCG	CAGGATGTAGGCGGTGGCTT
mABCG2	TCGCAGAAGGAGATGTGTTGAG	CCAGAATAGCATTAAGGCCAGG
mOCT4	AGCTGCTGAAGCAGAAGAGG	AGATGGTGGTCTGGCTGAAC
mSOX2	GCGGAGTGGAAACTTTTGTCC	CGGGAAGCGTGTACTTATCCTT
mAldh1a1	ATGGTTTAGCAGCAGGACTCTTC	CCAGACATCTTGAATCCACCGAA
mp53	TAACAGTTCCTGCATGGGCCGC	AGGACAGGCACAAACACGCACC
mPTEN	AGACCATAACCCACCACAGC	AGTGCCACGGGTCTGTAATC
mIL-17	ACCGCAATGAAGACCCTGAT	CAGGATCTCTTGCTGGATGAGA
mGAPDH	GGTGAAGGTCGGTGTGAACG	CCCGTAGGGCGATTACAGTC
hIL-17	CTACAACCGATCCACCTCACC	AGCCCACGGACACCAGTATC
hMMP2	TGAGCTATGGACCTTGGGAGAA	CCATCGGCGTTCCCATAC
hMMP9	CATCGTCATCCAGTTTGGTG	AGGGACCACAACTCGTCATC
hTGF-β1	GTACCTGAACCCGTGTTGCT	GTATCGCCAGGAATTGTTGC
hα-SMA	CATGGCATCATCACCAACTG	GCTGGGACATTGAAAGTCTC
hFibronectin	AGATGAGTGGGAACGAATGTCT	GAGGGTCACACTTGAATTCTCC
hVimentin	GCTGAATGACCGCTTCGCCAACT	AGCTCCCGCATCTCCTCCTCGTA
hGAPDH	GGAGTCAACGGATTTGGTC	GGCAACAATATCCACTTTACC

Supplementary Table 3. Correlation between expression of IL-17a and clinical pathologic features of NSCLC patients.

Characteristic	IL-17a		*P*-values
	Low (n=74)	High (n=42)	
Age			
≥50	43	23	
<50	31	19	
Gender			
Male	49	28	
Female	25	14	
Pathologic type			
Squamous cell carcinoma	42	20	
Adenocarcinoma	32	22	
Tumor size (cm)			
≥3	42	18	
<3	32	24	
Tumor location			
Left lung	36	22	
Right lung	38	20	
TNM classification			
T1	14	10	
T2	31	15	
T3	20	9	
T4	9	8	
Distant metastasis			
No	53	16	
Yes	21	26	